DEPARTAMENTO DE CIÊNCIAS DA VIDA

FACULDADE DE CIÊNCIAS E TECNOLOGIA
UNIVERSIDADE DE COIMBRA

"Intelligent design of color-tuned ChR2 variants for optogenetics applications"

Dissertação apresentada à Universidade de Coimbra para cumprimento dos requisitos necessários à obtenção do grau de Mestre em Biologia Celular e Molecular, realizada sob a orientação científica do Doutor João Peça (Centro de Neurociências e Biologia Celular) e da Professora Doutora Ana Luísa Carvalho (Departamento de Ciências da Vida, Faculdade de Ciências e Tecnologia, Universidade de Coimbra)

Bruno Filipe Pereira da Cruz

2014

DEPARTAMENTO DE CIÊNCIAS DA VIDA

FACULDADE DE CIÊNCIAS E TECNOLOGIA
UNIVERSIDADE DE COIMBRA

"Intelligent design of color-tuned ChR2 variants for optogenetics applications"

This work was performed at the Center for Neuroscience and Cell Biology, University of Coimbra, Portugal, with support from the Portuguese Foundation for Science and Technology (FCT) and FEDER/COMPETE with FCT grants: IF/00812/2012 and Pest-C/SAU/LA0001/2013-2014, and support from the Marie Curie Actions (PCIG13-GA-2013-618525) to João Peça; and FCT grant: PTDC/NEU-NMC/1098/2012 to Ana Luísa Carvalho

Bruno Filipe Pereira da Cruz

2014

Agradecimentos

Ao João Peça, orientador desta tese, queria agradecer a oportunidade dada de realizar este trabalho cientifico. Obrigado pelo apoio e compreensão ao longo deste ano, assim como as várias oportunidades que me foram dadas para ter contacto com tantas áreas distintas de investigação.

À Professora Ana Luísa Carvalho agradeço pela oportunidade e pelos conselhos dados para a realização desta tese.

I thank the Center for Computational Physics (CFC) of University of Coimbra for the opportunity to collaborate with them as well as the time spent teaching me about TD-DFT.

À Doutora Paula Verissímo e à Doutora Isaura Simões agradeco a prontidão na ajuda prestada na purificação da proteína assim como o acesso ao equipamento do seu laboratório, sem o qual este trabalho não poderia ter sido realizado.

À Professora Doutora Rosa Santos manifesto o meu agradecimento pela oportunidade de usar o equipamento de electrofisiologia.

À Ana Oliveira pela ajuda prestada nas experiências de electrofisiologia e por todos os conselhos dados, obrigado.

Um especial agradecimento aos membros do laboratório ALC, CBD e RDA pelo apoio prestado ao longo deste projecto.

Um agradecimento muito especial a Dona Céu e à Elizabete por manterem o laboratório “habitável” mas também por toda a ajuda e carinho demonstrado.

To the members of my group: Mr. Mo, Mário, Lara, Gladys and Fábio, for the countless talks, discussions and laughs shared, I express my deepest gratitude.

A todos os meus amigos, agradeço o apoio, carinho e as experiências partilhadas ao longo destes anos.

À minha família, em especial aos meus pais, agradeço todo amor, compreensão e confiança depositada em mim durante o meu percurso até este ponto.

Table of Contents

Summary

To better understand the neuronal system, beyond simply “listening” to cells one should be able to “communicate” with them. Until recently, approaches used to establish this communication while relying on the direct manipulation of neurons, have remained technically unsophisticated. Chemical and drug applications provide some degree of cell specificity at the cost of poor spatial and temporal resolution, while direct electrical stimulation of cells, even if allowing for more precise temporal control, lacks in cell type selectivity and may result in tissue damage.

In 2005, a new technical approach - Optogenetics - emerged as an answer to these limitations. Based on previously described proteins from the opsin family, such as Channelrhodopsin-2 (ChR2), several groups demonstrated that it was possible to directly manipulate neurons with light. These channels are capable of changing their permeability to certain ionic species upon illumination of specific wavelength and intensity. Using optogenetics, it became possible to activate discrete populations of neurons (-genetic) in a less invasive fashion using light (opto-), under precise temporal control (millisecond time scale) and high spatial resolution (fiber optical light spot).

For the past half-decade, great effort has been invested into improving the proprieties of these optogenetic channels and tools. Several enhancements have been achieved in terms of kinetics, for example: *Chronos,* ChETA and SFO variants; ion permeability: in the eNpHR 3.0 and iC1C2 variants; and in tuning the absorption spectra towards red-shifted variants as in: VChR1 and *Crimson*. This latter feature has taken up

great interest in the optogenetics field due to the scarceness of variants with non-overlapping absorption spectra.

With the recent determination of the crystal structure of ChR it is now possible to apply Time Dependent – Density Functional Theory (TDDFT) to predict the absorption spectra of the Channelrhodopsin using computational algorithms. Therefore, we propose to intelligently manipulate candidate residues to produce color-tuned variants of channelrhodopsin-2, taking advantage of TD-DFT calculations in order to predict the absorption spectra of these variants and, finally, using directed site mutagenesis to generate these mutants and to optimize their expression in a heterologous system.

This work describes the successful expression and purification of ChR2 in the *Pichia pastoris* expression system, and the generation and partial characterization of two novel ChR2 mutants. As a final goal, the determination of ChR2 absorption spectra was set, however, we could not achieve sufficient amount of protein for this analysis, and further optimization is required for the expression and concentration of purified protein samples. Further analysis using electrophysiology is also required to functionally determine the kinetic proprieties of the channel.

Keywords: Optogenetics; Channelrhodopsin-2; Red-shifted opsin; TD-DFT

Resumo

Para melhor compreender o sistema nervoso, para além de simplesmente “ouvir” as células, é também necessário “comunicar” com estas. Até recentemente, técnicas usadas para estabelecer esta comunicação eram caracterizadas pela sua falta de sofisticação técnica. Aplicação de drogas e outros químicos conferem alguma especificidade no que toca ao tipo de célula activada, no entanto, apresenta uma baixa resolução temporal e espacial. Por outro lado, electrofisiologia, apesar de permitir obter uma enorme resolução espacial e temporal, peca quando consideramos a especificidade celular obtida e a grande probabilidade de causar dano nos tecidos a serem estudados.

Em 2005, a técnica “Optogenética” emergiu como uma solução para os problemas técnicos apresentados anteriormente. Esta técnica baseia-se no uso de uma proteína da família das “opsinas”, “Channelrhodopsin-2” (ChR2), que vários grupos mostraram que é capaz de controlar actividade neuronal quando luz incide na mesma. Num mecanismo que envolve a captação de energia luminosa e convertendo-a em mudanças conformacionais da proteína, esta alterna entre estados permeáveis e não permeáveis, sendo possível controlar população geneticamente definidas (-genética) usando luz (opto-), com uma enorme precisão espacio-temporal.

Durante a última década, grande investimento foi desenvolvido no que toca a melhorar as propriedades deste canais “optogenéticos”. Grandes melhoramentos foram feitos relativamente a características cinéticas, por exemplo: Chronos, ChETA e variantes SFO; permeabilidade iónica: eNpHR 3.0 e iC1C2; e modificação do espectro

de absorbção para maiores comprimentos de onda: VChR1 e Chrimson. Esta última caracteristica têm gerado grande interesse na área já que, até à data, não existem variantes que não apresentem espectros de absorção totalmente distintos.

Com a recente determinação da estrutura da ChR é possível aplicar teorias de mecânica quantica como “Time Dependent – Density Function Theory” (TD-DFT) para prever o espectro de absorpção da proteína usando métodos computacionais. Assim, propomos mutar, intelegetemente, resíduos na proteína de forma a obter variantes que respondam a maiores comprimento de onda, tirar partido de TD-DFT para prever os seus espectros e finalmente validados em laboratório, expressando estas variantes num sistema heterologo.

Esta tese descrever a expressão e purificação de ChR2 no sistema heterologo de Pichia pastoris. Como objectivo final, a determinação do espectro de absorção da proteína foi delineado, no entanto devido à baixa quantidade de proteína isolada tal não foi possível e assim futuras optimização ao protocolo serão necessárias, assim como várias outras análises, nomeadamente no que toca as propriedades cinéticas da proteína usando técnicas de electrofisiologia.

Palavras-chave: Optogenética; Channelrhodopsin-2; opsina “red-shift”; TD-DFT

Chapter I – Project motivations and objectives

Project motivations and objectives

The daunting task of studying the animal brain has always been hindered by its sheer complexity. A major goal in neuroscience has been to look for approaches that allow the dissection of the individual pathways that drive neural communication between nervous cells. To do so, it is essential to employ tools capable of exerting high spatio-temporal control over neurons and that are capable of supplanting the limitations of methods such as electric and chemical stimulation.

Recently, a protein identified from the algae *Chlamydomonas reinhardtii,* channelrhodopsin-2 (ChR2) was engineered to allow for precise control of neural cells. Although light-responsive proteins have been known for some time, ChR2 was the first single protein system to successfully drive neuronal activation upon light excitation with high temporal resolution. This protein is comprised of 7 transmembrane α-helix domains with a covalently linked retinal molecule that functions as its chromophore (i.e. absorbs photons with energy in the visible spectra). When light is captured by ChR2, the retinal molecule undergoes a conformational change that allows the protein channel to adopt a conducting state that is permeable to several ionic species. When this protein is ectopically expressed in neurons, this ionic diffusion results in depolarization of the cell membrane and consequent generation of action potentials. The application of ChR2 in neurobiology was seminal to what is now known as “optogenetics”. This new field comprises a toolbox with an ever-growing repertoire of molecular actuators, fluorescent sensors, and activity indicators.

Notwithstanding the scientific progress made by the use of these tools, there is still room for greater improvement. For example, one of the key limiting features of ChR2 is its absorption spectra, which presents a peak absorption near 470nm (blue light). The lack of a red-shift alternative complicates the use of ChR2 for deeper tissue stimulation and, most importantly, precludes its use for the distinct excitation in spatially overlapping neuronal population.

Nevertheless, because the structure of ChR was recently resolved by X-ray crystallography, it is now possible to apply quantum physics theories, such as TD-DFT, to determine the influence of the electrostatic environment around the retinal molecule on its absorption spectra. This can be achieved through a simulation of mutations on the primary structure of the protein, and determining, *in silico*, the absorption spectra of a given ChR2 variant.

This project is centered on validating the theoretical predictions provided by the Center for Computational Physics (CFC) of University of Coimbra, by means of protein production and purification as well as cellular and biophysical characterization of the generated mutants.

Such validation will result in a method to generate, on demand, color-tuned ChR2 mutants with scientific and biomedical applications. Moreover, this work might open the avenues, through the application of the same rational; to obtain color tuned variants of a virtually endless array of molecules.

Chapter II – Theoretical background

Theoretical background

II.1 - Channelrhodopsin-2 as a molecular tool for optogenetics

II.1.1 – The Opsin Family

One of the most amazing features developed during the course of evolution was the ability of organisms to perceive light. Perception of light and its constituent colors, as changes in visible electromagnetic radiation, enables organisms, from single cell algae to mammals to perceive and respond to environmental cues and to adjust their behavioral responses.

Although many different strategies are employed in nature to allow for this detection, most, if not all, fall into the absorption of quanta of light, i.e. photons, by a biomolecule (e.g. chromophore), resulting into downstream signaling, with a final behavior response from the organism. One of the most abundant and conserved family of proteins involved in the process of photodetection is the retinylidene protein family (commonly called opsins). These proteins are characterized by a seven-transmembrane structure with a covalently linked retinal residue (the molecular complex of retinal plus opsin is called rhodopsin).

In humans, visual perception is possible because of the expression of members of this family, type II rhodopsins, in a specialized subset of cells in the retina. Upon receiving light and consequent photoisomerization of 11-cis retinal into all-trans retinal, these proteins suffers several conformational changes allowing protein-protein interactions with their downstream target protein - *transducin*. The latter, through the

interaction with several other proteins, provokes membrane hyperpolarization in the photoreceptor cell (e.g. rod cells) [1].

A distinct type of rhodopsins (type I) found in lower level organisms (e.g. prokaryotes, algae and fungi) are also responsible for photon absorption. Contrary to the type II rhodopsins, which replace the retinal from the biding pocket upon light-induced isomerization, type I rhodopsins are characterized by the induction of photoisomerization of retinal - from all-trans to 13-cis - and subsequent regeneration of the molecule to all-trans confirmation. Moreover, another key difference resides in the mechanism by which the protein signals, as type I rhodopsins directly influences the membrane potential of the cell, or organelle, by functioning as a light-gated ion channels (or in some cases ionic pumps).[2]

II.1.2 – Microbial rhodopsins

In the 17th century, Treviranus described, for the first time, the effect of light exposure on the motile behavior of certain species of algae[3]. This effect - phototaxis - was defined as the parallel orientation that some organisms assume relative to a light source, which can be positive or negative phototaxis depending if the organism moves towards or away from the light, respectively. This phenomenon was further characterized by Buder one century later[4]. He found that a wide variety of algae (e.g. *Chlamydomonas* and *Carteria*), upon illumination from a steady light source, positioned themselves parallel to the direction of the light. Buder hypothesized that this could be a biologically relevant behavior (Fig.1). Later studies also implicated cations, namely Ca^{2+}, to be essential to this mechanism[5]. Recently, Peter Hegemann's group recorded photocurrents from *Chlamydomonas* algae leading to the proposal that due to the small delay between photostimulation and the currents observed, the proteins responsible for this response to light were, most likely, spatially connected or even function as single protein channels that would become permeable to discrete ionic species upon illumination[6]. Using bioinformatics, several more species have been identified as having rhodopsin-like sequences on their genome. Interestingly, even some prokaryotes express a form of rhodopsin, Bacteriorhodopsin (BR), which act as a proton-pump when illuminated[7]. More recently, Nagel et al recorded, for the first time, photocurrents of this protein under voltage-clamp conditions by expressing the protein in *Xenopus laevis*' oocytes[8].

With the advent of cDNA libraries and using information from previously known opsins, novel sequences encoding for unknown "type-1 like-rhodopsins" have been

identified. Among the newly discovered protein sequences were ChR1[9] (ChannelRhodopsin-1) and ChR2[10] (ChannelRhodopsin-2) proteins from *Chlamydomonas reinhardti*.

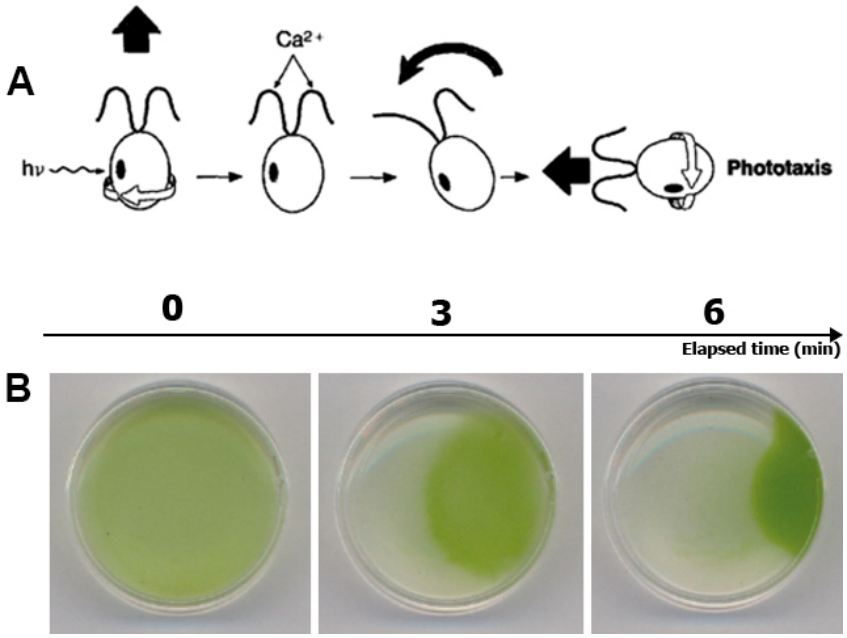

Figure 1 - Phototaxis in *Chlamydomonas* algae. a) schematics of the influence of light on the movement of a single cell: the light shines on the eye-spot, opening the channelrhodopsin channel and allowing for an influx of calcium that signals the algae to move towards or away from the electromagnetic radiation (from [11]). b) phototaxic movement of *Chlamydomonas* wild type strain, in culture, when exposed to light (from [3])

II.1.3 – Historical perspective on Optogenetics

Following the hypothesis that bacterial and algal rhodopsins could be used as molecular tools to depolarize other biological systems, in the same paper describing the biophysical proprieties of ChR2[10], Nagel et al demonstrated that it was possible, not only to express this protein in mammalian cells (HEK293 and BHK cell lines), but that it was also was possible to achieved light-induced depolarization[10].

Based on these observations, these same tools could be used in other areas, such as neuroscience. As neurons are intrinsically excitable cells, (due to their ability to respond to changes in membrane potential) it was thought that the same molecular tool that was used to change the membrane potential in kidney cell lines, could also be applied to drive activation, i.e. generate action potentials in neurons or even other types of excitable cells[12]. Pursuing this idea, in 2005, seminal papers describing the activation of neurons using ChR2 were published by Karl Deisseroth's group[13],[14].

Because it allows the manipulation of the cell using light (opto-) and because it is possible to encode the protein as DNA and to control its expression using specific promoters (-genetic), the term optogenetics became popular to describe this technological approach[15].

More recently, and propelled by the recently resolved crystal structure of ChR (C1C2)[16], the field of optogenetics has grown from the development of new, and improved tools. Presently, desirable variants of opsins include channels that display greater single channel conductance, faster/slower kinetics (e.g. ChETA mutants allowing for ultra-fast excitation and SFO allowing for stable and long-lasting

depolarization over long periods of time), different times of desensitization and selective permeability to a given ion are some examples[17].

Concurrently, since these proteins are mostly derived from lower eukaryotic or even prokaryotic organisms, optimization of expression through the “humanization” of codon sequences has been employed to increase the expression of these proteins in mammalian cells. Additionally, the insertion of discrete trafficking signals in the coding sequence of optogenetic tools, has allowed for the optimization of their delivery to the cell membrane[18].

Finally, the need to increase the range of available wavelengths to activate the opsins, has resulted in the identification of variants with a slight red-shifted activation spectra in *Volvox carteri* (VChR1 and VChR2). However, the absorption spectra of these variants are, to a great extent, overlapped with the spectra of the original, and widely used, ChR2 (Fig.2). More recently, Boyden and colleagues by screening a considerable amount of different algae species, identified a new red-shifted variant named *Chrimson* with a peak absorption of 590nm, unfortunately its kinetic parameters are still far from desirable when compared to ChR2 and it is still activated at 470nm, albeit to only a fraction of its peak currents[19].

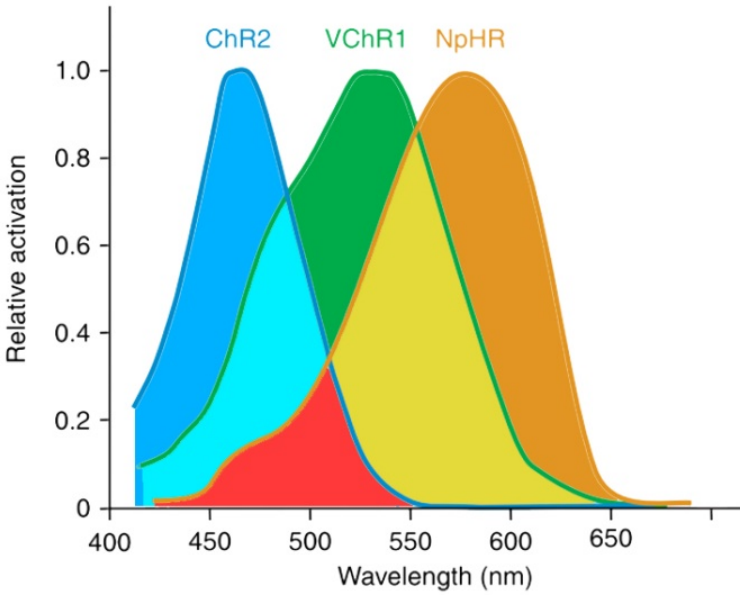

Figure 2 - Action spectra of ChR2, VChR1 and NpHR. ChR2 displays an absorption peak at approximately 470 nm, VChR1 peak is red-shifted to 535 nm while the chloride pump NpHR absorbs maximally at 590 nm. There is significant overlap in the absorption spectra of ChR2 and VChR1 (in cyan), between VChR1 and NpHR (in yellow) and between the three opsins (in red). Adapted from [20].

II.1.4 – Structure and function of Channelrhodopsins

Currently, Channelrhodopsins (ChR) are the only known proteins channels directly gated by light. They are part of the microbial, type I rhodopsins found in several types of organisms ranging from archaea, eubacteria, fungi to algae. The next section focuses on key aspects of the structure and mechanism of action of these proteins as well as the rationale behind some of the most important engineered variants presently available.

Protein Structure

Channelrhodopsins are protein channels that span across the cell membrane with a seven-transmembrane α-helix topology (7-TM). Furthermore, all known Channelrhodopsins (in fact, all rhodopsins) have another common feature in their structure: a retinal molecule (RET) covalently linked to an amino acid (a.a) residue, the former acting as Schiff base connecting to the protein backbone through a N=C bond. This prosthetic group is responsible for the absorption properties of the protein in the visible range of the electromagnetic radiation spectra. Both the maximal extinction coefficient, ε, and quantum efficiency, Φ, present relatively high values for a biologic molecule (ε=50,000$M^{-1}cm^{-1}$; Φ= 30-70%)[21]. However, as this property is intrinsic to the retinal molecule it is challenging to improve this characteristic. On the other hand, the possibility of modifying the absorption spectra of the opsin, by modulation the electronic environment in which the retinal molecule is inserted represents a good target for protein engineering approaches.

Interestingly, both retinal and the protein, when isolated, absorb primarily in the near-UV range (RET's λ_{max}=380nm) however, when bound together, the protein pocket, that houses the retinal molecule, induces a red-shift in the retinal's absorption spectra, an effect known as "opsin shift"[22]. It is known that the absorption of the retinal molecule is due to the π-conjugated polyene chain, that allows electrons to transit between π→π* with an energy gap corresponding to visible radiation (400~700nm)[23]. Although not fully understood, it is thought that this shift results from the conformational manipulation of the chromophore as well as the direct electrostatic interactions established between the nearby protein residues and RET[24].

When cloned for the first time from *C. reinhardtii*, ChR2 was identified as consisting of 737 amino acids comprising a 7-TM domain (~300a.a), with some sequence homology with the proton pump BR, and a ~400 a.a. region in the C-terminal proven to be non-essential to the light gated proprieties of the channel[10]. Most variants of ChR2 used for optogenetics proposes lack the original C-terminal domain (Fig.3).

Because bovine Rhodopsin[25] and BR[26] were the first rhodopsins with their crystal structures resolved, the initial approaches to understand the structure of channelrhodopsin were approximated through sequence comparison, homology models and structure refinement using bio-computational techniques[22]. Despite its helpfulness, newer, more accurate, models are still required, potentially using more refined techniques such as *ab-initio* designs. In 2011, a projection of ChR2 was published[27] and finally in 2012, H. Kato et al. [16], reported the first crystal structure of ChR from a chimeric version of ChR1 and ChR2 (C1C2 chimera). This was the first model revealing the conformation of the channelrhodopsin light-gated cation channel.

```
1   MDYGGALSAVGRELLFVTNPVVVNGSVLVPEDQCYCAGWIESRGTNGAQT
51  ASNVLQWLAAGFSILLLMFYAYQTWKSTCGWEEIYVCAIEMVKVILEFFF
101 EFKNPSMLYLATGHRVQWLRYAEWLLTCPVILIHLSNLTGLSNDYSRRTM
151 GLLVSDIGTIVWGATSAMATGYVKVIFFCLGLCYGANTFFHAAKAYIEGY
201 HTVPKGRCRQVVTGMAWLFFVSWGMFPILFILGPEGFGVLSVYGSTVGHT
251 IIDLMSKNCWGLLGHYLRVLIHEHILIHGDIRKTTKLNIGGTEIEVETLV
301 EDEAEAGAVP
```

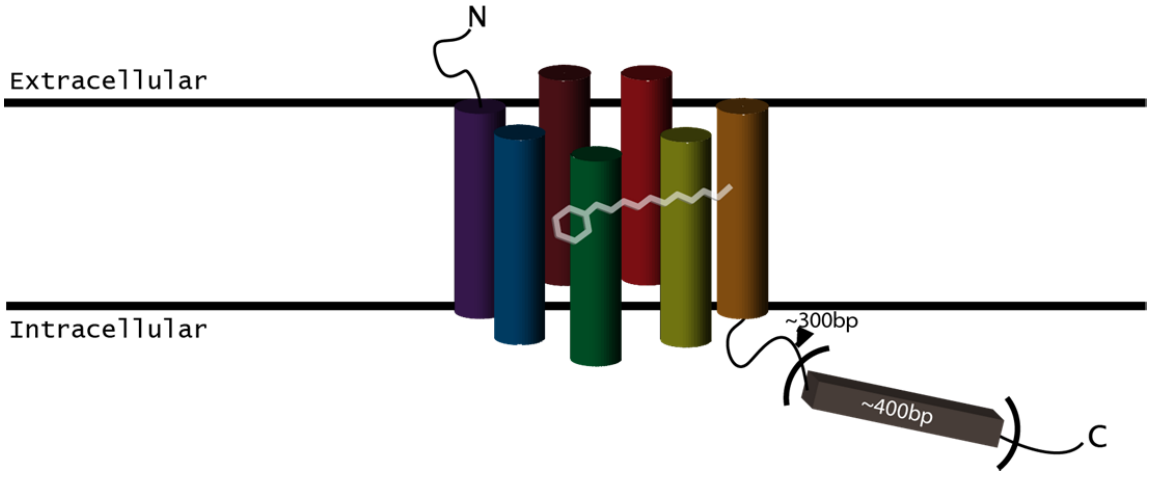

Figure 3 - Sequence of humanized ChR2 (hChR2) and the standard membrane topology of ChR. Black arrow indicates where the ChR2 variants, used in optogenetics, are truncated in relation to the ChR2 initially identified in *C. reinhartii*. Highlighted sequences represent the transmembrane domains based on the C1C2 published structure[16].

The retinal-binding pocket

As mentioned above, all rhodopsins share as a common feature the presence of a retinal molecule covalently linked to the protein structure. In the case of type I rhodopsins, this link is possible due to a Lysine residue (K257) present in the seventh transmembrane helix (TM7), which is highly conserved in this sub-family (from this point on all the residue numbering between parenthesis refers to ChR2 sequence in Fig.3),. Additionally, five aromatic residues (Trp124, Phe178, Trp223, Phe226 and Phe230) (Fig.4d), located near the aliphatic RET chain stabilize the RET molecule forming the hydrophobic pocket. Furthermore, the residues Cys128, Thr159, Ser256, Gly181 and Glu123 (Fig 4e) are thought to be responsible for the "opsin shift" by creating a "less-hydrophobic" pocket, as well as being responsible for some kinetic properties of the channel[16,21,22]. Finally, Asp253 has been identified as a proton acceptor to the Schiff base because of its proximity to Lys257 and the abolished photocurrents resulting from directed mutagenesis experiments on the C1C2 chimera[16].

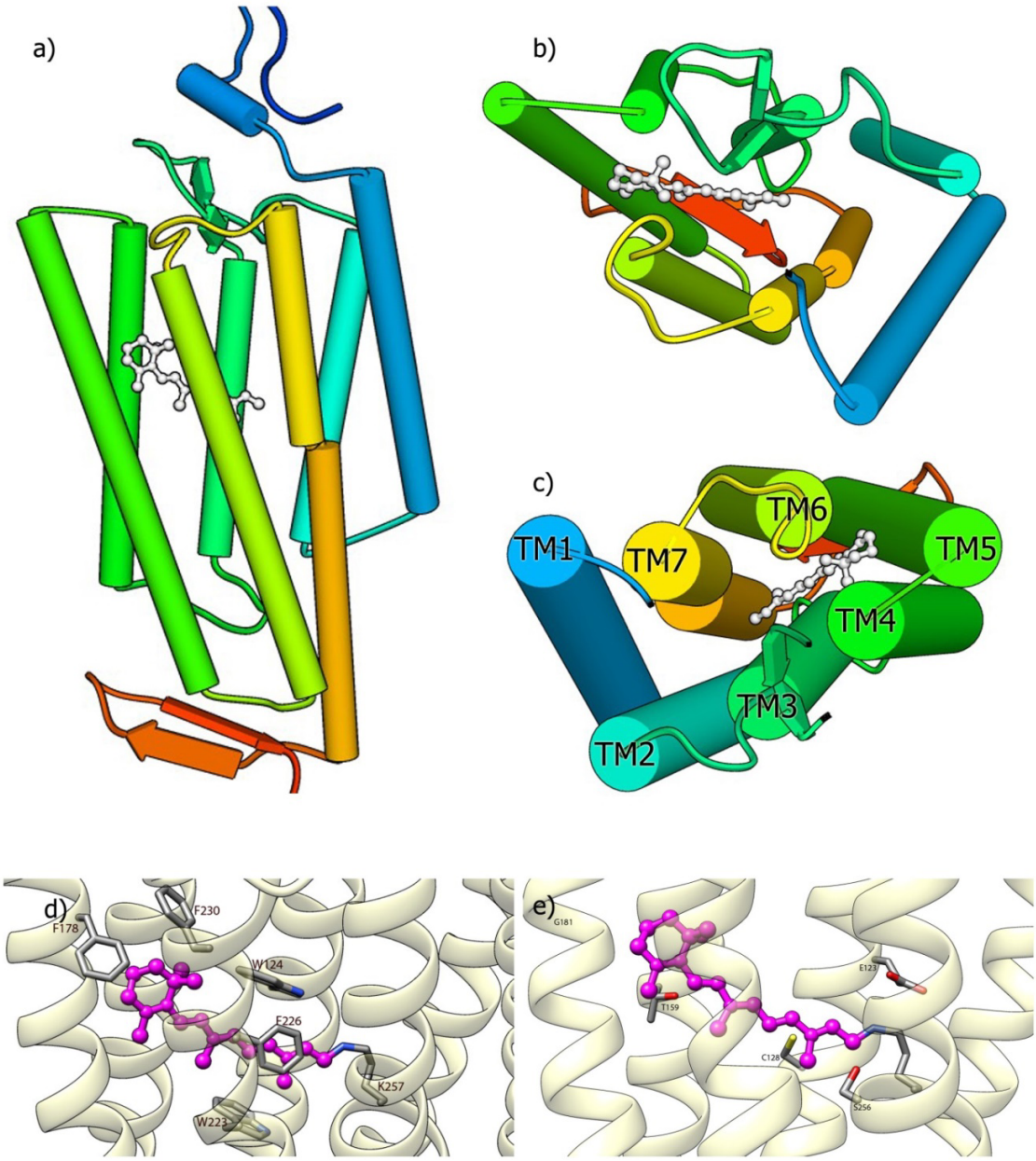

Figure 4 - Crystal structure of ChR as determined by H.Kato et al. (pdb : 3ug9). a) side view; b) top view; c) top view with identified transmembrane domains as in Fig.3, d) aromatic residues forming the retinal pocket; e) residues though to be responsible for the opsin-shift in the retinal absorption spectra. The numbering on the images is according to ChR2 sequence in Fig.3.

The ion pore

Contrary to what occurs in mammalian rhodopsins, Channelrhodopsins display intrinsic ion channel activity. From what we have learned from other cationic channels, in order to have a pore capable of transporting ion species, these must be stabilized by electrostatic interactions[28]. As ChR is more permeable to cations than anions, a highly electronegative region is expected to form the pore through which the positively charged ions would travel. Previous reports have identified Glu90[29], Glu97, Glu101[22], Asp156, Asp253, His134 and Glu123[21] as important residues for the kinetic proprieties of the protein, specifically by being part of the ion channel. Using the C1C2 structure, H. Kato et al, found a candidate electronegative region formed by TM1, 2, 3 and 7 where polar residues (Gln56, Thr59, Ser63, Glu83, Glu90, Lys93, Glu97, Glu101, Glu123, Thr246, Asp253 and Asn258) (Fig.5), turned to the inside of the protein, appear to come together to form a strong electronegative and hydrophilic surface that could be responsible for the stabilization of cation species, further evidence of their importance comes from mutagenesis studies in the same paper, where swapping some of the residues previously mentioned causes a loss in ion selectivity and conductance[16]. Additionally, a ChR2 study using bioinformatics modeling of ChR2 mutants, indicate that in addition to Gln56 and Ser63, Thr250 and Asn258 residues might play a role in channel selectivity.[30]

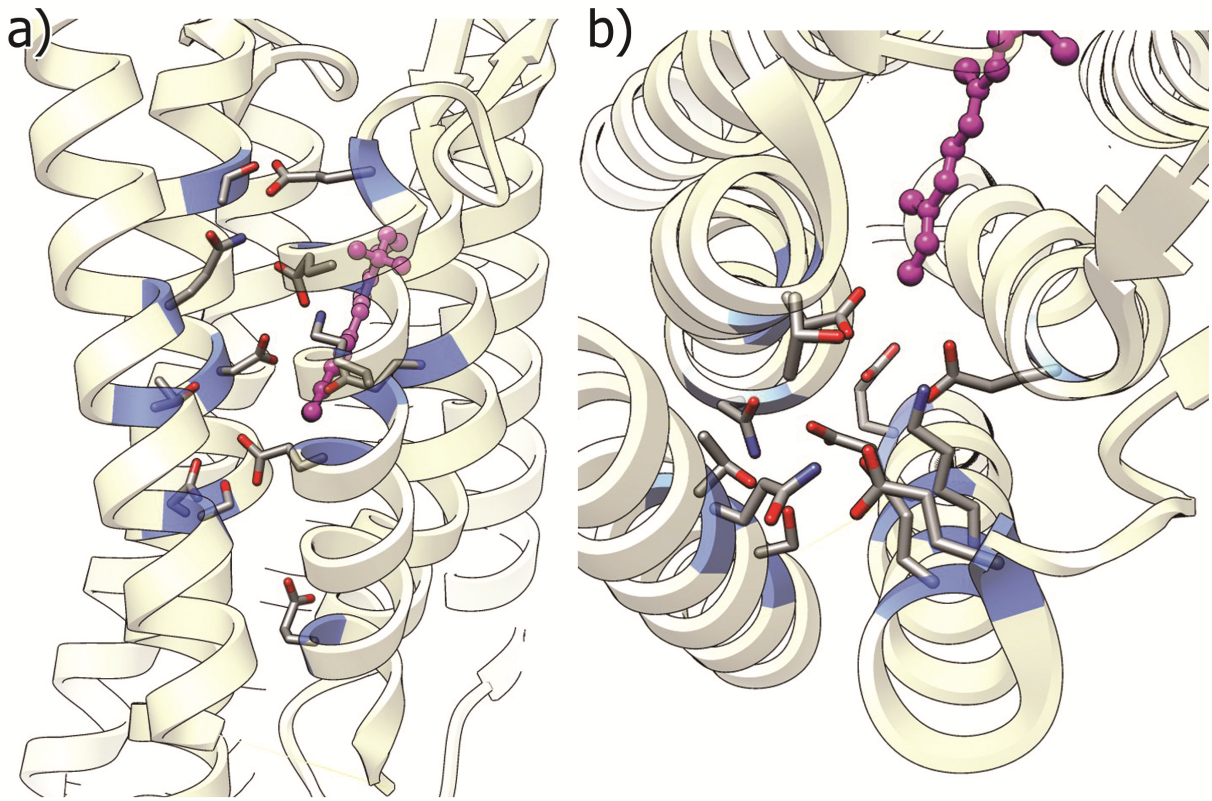

Figure 5 - Residues forming the negative pore in ChR (pdb : 3ug9) responsible for ion transport. a) side view; b) top view. Retinal in purple; oxygen atoms in red; nitrogen atoms in blue. The blue color in the backbone represents the backbone portion of the amino acids forming the channel.

ChR2 photocycle

When inserted into the cell membrane of neurons, ChR2 is capable of eliciting action potentials[10]. This activity is possible because under appropriate lighting, ChR2 can undergo change in conformation to become permeable to a broad range of ionic species[10]. The molecular mechanisms controlling changes in permeability and the sequence of structural changes the channel undergoes, as a reaction to incident light, is known as the photocycle[31]. Several models of this mechanism have been suggested, however the one that gathers more consensus is the six-state photocycle model proposed by Ritter et al. in 2008[32]. According to this study, ChR2, when in the dark, exists as a non-conductive and excitable form with a maximum absorption peak of 470nm (D470)[32]. This state is readily converted (in approximately 1ms[33]) to a conducting state with its peak absorption at 520nm (P520). Between these two states, other two very fast intermediates, without measurable currents, are present: P500, resulting from the very fast photoisomerization of retinal (Fig.6b), and P390 which is the product of the Schiff base deprotonation. After deprotonation, the protein undergoes severe conformation changes acquiring the P520 conducting state. As mentioned above, the open state of ChR2-WT lasts for around 10ms, after which the protein decays into a P480 state (under special circumstances the P520 can be directly converted to D470)[32]. Since this is the slowest step of the cycle, under continuous light conditions these intermediates are accumulated and give rise to a light adapted form of ChR2. The P480 state can be further divided into two sub-states differing in their excitability to light. P480a is created from P520 and cannot be directly “reactivated” by

light. On the other hand, in an equilibrium with the “a” state, is the “b” state that is, in turn, is activated by light of 480nm (P480->P500). This specie can also complete the photocycle by the recovery of the dark-state D470[32],[33]. Although not fully understood, it is possible that some of the conversion steps have shortcuts, loops and even different kinetics (Fig.6a). For example, SFO mutants seem to be able to remain in the P520 state for periods of time up to 30 minutes in some ChR2 variants. This intermediate can therefore maintain steady state currents and because they occupy this conformation for longer periods of time, the shortcut P520-D470 becomes interesting since it allows for a direct ablation of currents using precise optical control[2]. On the other hand, ChETA variants seem to have a faster recovery from the P520 to P480 state which results in a much faster reactivation, allowing for better temporal resolution and faster channel kinetics[34].

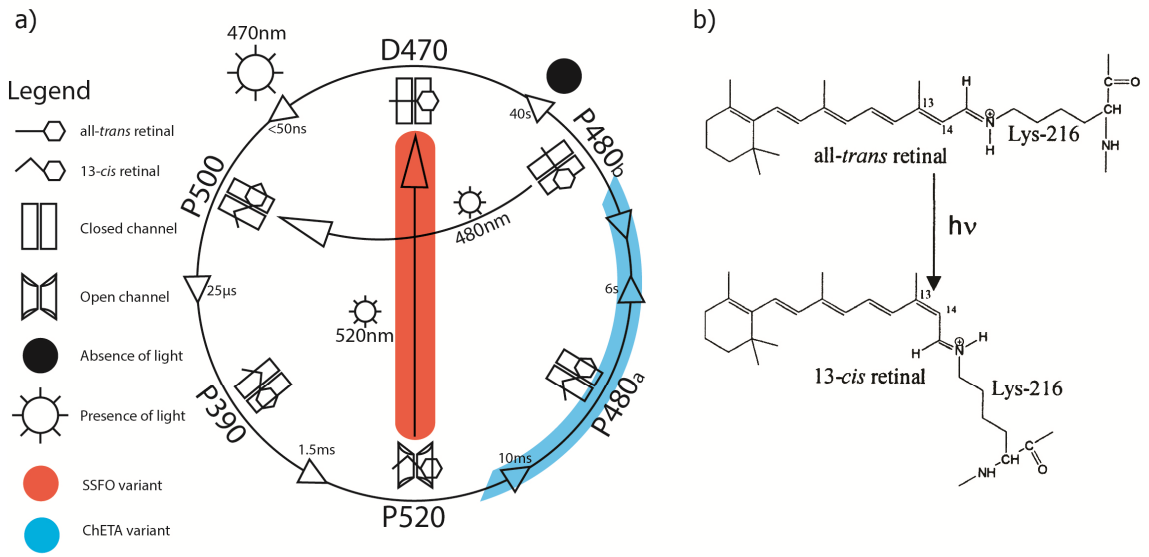

Figure 6 - ChR2 photocycle according to the six-state model. a) Diagram depicting the changes in the protein during ChR2 photocycle, and the relaxation time constants of the protein's states (adapted from 41). b) photoisomerization reaction of all-*trans* retinal into 13-cis retinal.

II.1.5 – Towards a red-shifted Chanelrhodopsin-2

In previous sections we discussed the structure and function of ChR2, as well as the interest in red-shifted depolarizing tool with kinetic characteristics similar to the wild-type protein. In the next section we review some of the most important milestones achieved regarding the manipulation of ChR2, its rational, applications and contribution for the generation of a red-shifted opsin.

As mentioned before, Nagel et al [10], took the first step towards using ChR2 in a heterologous system to achieve cellular depolarization. In this seminal paper, a thorough description of the channel's kinetic proprieties was performed. Channelrhodopsin-2 was shown to display permeability to a broad array of positive ions with conductance inversely dependent to ionic species radius. Most importantly, it was shown that ChR2 expression is enough to generate mammalian cell depolarization without the need for added soluble factors. This is in contrast to other mammalian rhodopsins where signal transduction results from a long cascade of protein-protein interactions [35].

In subsequent experiments, Boyden et al [14], expressed this same protein in neurons, proving for the first time that is possible to drive neuronal firing with a single

spike fidelity of up to 30Hz without significantly affecting the resting proprieties of the neuron cell (membrane resistance, resting potential and spikes evoked by current injection). This work also suggested for the first time, the potential of using ChR2 in combination with other molecular tools, e.g. cell-specific promoters, and potential *in vivo* applications. Soon after this work the first transgenic mice models of ChR2 were developed in Guoping Feng's laboratory and applied to the study on neuronal circuitry in vivo[36].

While neuroscience was taking the first steps to make this opsin the widely used tool that it is today, other groups interested in the biophysical properties of these proteins, also contributed with key findings. The first paper describing structural features and the photocycle of ChR2 came from Ernst Bamberg's group. Due to the specific biochemical nature of these experiments, the need for a pure protein sample was present. As a result this was also one of the first studies describing the process for production and purification of Channelrhodopsin-2 using *Pichia pastoris* as the chosen expression model, in order to obtain an absorption spectra of the protein[33].

Taking the first step towards a red-shifted ChR, Zhang et al[37] characterized VChR1, a channelrhodopsin that shows a 70nm shift, resulting in yellow light excitation. Due to high resemblance in the primary structure between VChR1, ChR1 and Chr2, comparison of their sequences revealed several candidate residues responsible for the color-tuning of the protein's absorption spectra. Against what had been previously hypothesized, these residues were not involved in the counter-ion complex of the Schiff base, in fact, they were located in the TM5 of the proteins structure in close proximity to the β-ionone group of the retinal molecule. These substitutions (glycine 182 and

cysteine 184 by serines) resulted into a more polar electronic environment on the retinal molecule and ultimately leading to a red-shifted absorption spectra, suggesting the possibility of color-tuning by modification of the protein's primary structure.

Later, by comparing ChR2 sequence to Bacteriorhodopsin, André Berndt et al[38] identified the C128 residue as a potential target for mutation resulting into slower channel kinetics. In fact, by following what had already been done in a homolog residue of BR[39], substitution of this cysteine by a serine or alanine, resulted into bi-stable opsin that could be turned on/off with distinct wavelengths. This tool was later improved by a synergistic effect between, the previously identified mutation, C128S and D156A resulting into an closing constant of 30min[40] making it possible to optically control the overall excitation state of a given neuronal population for long periods of time. These variants were extensively characterized by structural methods using, once again, *P. pastoris* as the chosen model of expression[41].

Several papers unveiling the properties of ChR2 structure and function have been published published. Among these we highlight: a proposed structure of ChR2 using CrioEM[27] and the study of molecular mechanism governing the ion channel selectivity[29]. Hideaki E. Kato *et al*[16] published the crystal structure of C1C2, a chimera between ChR1 and ChR2, delivering the first high resolution model. This study allowed the determination of both the retinal binding pocket and ion pore with greater confidence, opening the doors to intelligent design approaches based on the 3D structure of the protein. Interestingly, in this study the authors opted to use a different expression model, making use of Sf6 insect cells to express the protein, albeit maintaining the overall purification strategy.

The seminal study by Wang *et al*[24] reported the color-tuning of all-*trans* retinal in a protein environment. Using a modified human cellular retinol binding protein II (hCRBPII) , thought to be responsible for the transport of retinal, binding it in a similar way to mammalian rhodopsins, to demonstrate the possibility of mutating several residues on the protein to yield peak absorption shifts on the retinal molecule, ranging from 440 to 644 nm (Fig. 7). Moreover, by studying the structure of the protein relative to the retinal molecule they concluded that modifications that isolate the retinal molecule into a hydrophobic environment and even the electronic charges in the polyene chain, especially near the protonated Schiff base (PSB), resulted into greater bathochromic shifts than modifications near the β-ionone ring, a result contradicting the findings regarding VChR1. However, due to the differences between Channelrhodopsins and hCRBPII, especially in the PSB motif, it is possible that these reports are not directly comparable.

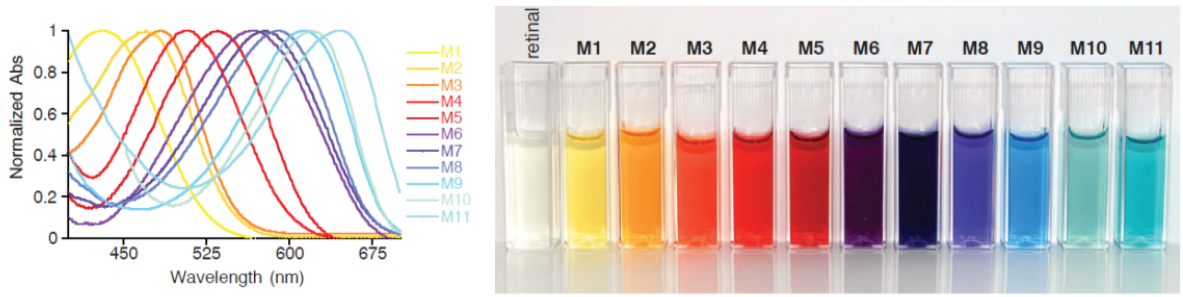

Figure 7 - Rainbow-like absorption spectra in a modified retinal binding protein. Seminal example of color-tuning of hCRBPII using a directed site mutagenesis strategy aimed at modifying electrostatic environments surrounding the retinal molecule. From [24]

More recently, two breakthroughs have been made in the field of Channelrhodopsin engineering. By taking a similar approach to the discovery of VChR1, Nathan Klapoetke *et al*[19], screened over a hundred species of algae for "Channelrhodpsin-like" sequences. After expressing, and testing the photoconductances of the several candidates, two interesting new opsins were discovered: *Chronos* (from *Stigeoclonium helveticum*), a blue-light sensitive high frequency actuator similar to previously engineered ChETA variants, and *Chrimson* (from *Chlamydomonas noctigama)* the first identified variant with a yellow peak absorption (590nm). Due to kinetic issues (low spike fidelity over 10Hz), several mutants were screened to yield a final *ChrimsonR* (K176R mutant) which presents a more suitable off-kinetic curve, similar to the commonly used ChR2. Unfortunately, this opsin still presents blue-light sensitivity, making difficult to achieve true independent neuronal excitation under normal circumstances, when paired with ChR2

Finally, Deisseroth and collaborators[42], using published structure of C1C2 , turned the channelrhodopsin into a chloride permeable pore through several rounds of directed-site mutagenesis, turning the depolarization tool into a neuronal silencing actuator. By identifying the ion pore positive residues responsible for the cation stabilization and modifying its charges, replacing them by positive or uncharged amino acids, a variant with nine modifications (iC1C2) was shown to have a reverse potential close to the theoretically predicted for the chloride ion. Moreover, applying the previously engineered strategy used in the SSFO variants, mutation of a homologous residue in the iC1C2 structure yielded a bi-stable chloride channel, albeit with a small τ-off constant compared to the ChR2-SSFO variant. This example and past work

emphasize the possibility of altering several amino acids in ChR structure without leading to a functional impairment of the protein, evidencing another feature of the protein that facilitates its engineering.

Channelrhodopsin-2, and its variants, have proven to be a great asset to the neuroscience field[43]. When genetically encoded into neurons, these proteins, allow for, optically controlled activation of cells with a sub-second time scale resolution[44]. Table 1 and Fig. 8 provide an overview of the available and most widely used opsins in the field of optogenetics as well as their most relevant features.

Even though recently developed, optogenetics has evolved rapidly. Nevertheless, several issues remain to be solved. Apart from the recent kinetic variants of ChR2 (ChETA and SFO(s)) producing successes into novel scientific paradigms, not many advances have been made regarding other protein proprieties. The need to selectively activate more than one neuronal population occupying the same area, and other technical considerations (e.g. red-shifted light activation results in less tissue damage and higher penetration of radiation), calls for the development of color-tuned variants of ChR2 with distinct activation spectra. Genome-mining approaches have resulted in the identification of several ChR-like proteins (e.g. VChR1, *Chronos* and *Chrimson*), but these do not yet cover the entire spectrum of desirable properties. With the current knowledge of ChR structure, it is now possible to intelligently manipulate the primary structure of the protein with the aim of obtaining new variants with desired proprieties. Moreover, the validation of our directed color tuning approach can provide information that can be applied to other proteins.

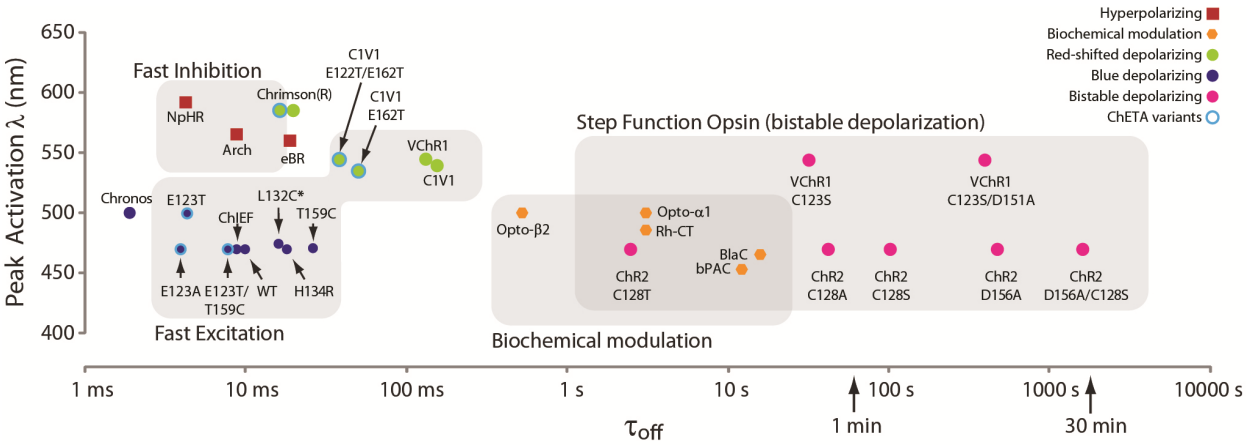

Figure 8 - Spectral proprieties and off kinetics of several published opsins. In the highlighted region (>500 nm peak activation) mostly slow kinetic depolarizing opsins are present (>50 ms t_{off}). Most red-shifted opsins are hyperpolarizing pumps (NpHR and Arch). For depolarizing tools there is a tradeoff between kinetics and peak activation. Adapted from [45]

Table 1 – Most widely used current optogenetics actuators for neuroscience applications

Abbreviation	Wild-type designation	Peak activation wavelength (nm)	τoff (ms)	Channel Permeability	Effects on neurons	Reference
Wild type opsins						
ChR1	Channelrhodopsin-1	495	49d)	H+	Dp c)	9
VChR1 a)	Channelrhodopsin-1	535	133	H+	Dp	37
MChR1 b)	Channelrhodopsin-1	540	27	Cations	Dp	46
ChR2	Channelrhodopsin-2	470	13	H+.Na+.K+.	Dp	10
NpHR	Halorhodopsin	590	3.6	Cl- (Pump)	Hp	47
Chronos e)	ShChR	500	21.4	H+.Na+.K+.	Dp	19
Chrimson f)	CnChR1	590	41	H+.Na+.K+.	Dp	19
Arch	Archaerhodopsin-3	566	19	H+(pump)	Hp	
Engineered opsins						
ChR2-H134R	ChR2 mutant	470	18	H+.Na+.K+.	Dp	48
ChR2-T159C	ChR2 mutant	470	26	H+.Na+.K+.	Dp	43
ChR2-L132C	ChR2 mutant	474	16	H+.Na+.K+.	Dp	43
ChEF	ChR1/ChR2	470	26	H+.Na+.K+.	Dp	49
ChIEF	ChR1/ChR2	450	10	H+.Na+.K+.	Dp	49
C1V1	ChR1/VChR1	540	156	H+.Na+.K+.	Dp	40
C1V1 (E162T)	C1V1 mutant	530	58	H+.Na+.K+.	Dp	40
C1V1 (E122T/E162T)	C1V1 mutant	535	34	H+.Na+.K+.	Dp	40
ChETA(E123T)	ChR2 mutant	490	4	H+.Na+.K+.	Dp	49
ChETA(E123A)	ChR2 mutant	470	4	H+.Na+.K+.	Dp	49
ChETA(E123T/T159C)	ChR2 mutant	490	8	H+.Na+.K+.	Dp	49
ChR2-SFO (C128T)	ChR2 mutant	470//590 e)	2s	H+.Na+.K+.	Dp	38
ChR2-SFO (C128A)	ChR2 mutant	470//590 e)	42s	H+.Na+.K+.	Dp	38
ChR2-SFO (C128S)	ChR2 mutant	470//590 e)	1.7min	H+.Na+.K+.	Dp	38
ChR2-SFO (D156A)	ChR2 mutant	480//590 e)	6.9min	H+.Na+.K+.	Dp	40
ChR2-SSFO	ChR2 mutant	470//590 e)	29min	H+.Na+.K+.	Dp	40
eNpHR 3.0	NpHR mutant	590	4.2	Cl- (Pump)	Hp	50

Dp = Depolarization, Hp = Hyperpolarization, a) Isolated from *Volvox carteri*; b) Isolated from *Mesostigma viride*; c) under physiologic pH the amount of protons that permeate the channel are not sufficient to drive action potentials; d) measured at 30ºc and pH 4; e) SFO = Step function opsins, these opsins have very slow kinetics and can be inactivated using a second wavelength. E.g. using 470nm to open the channel and 590 to close it. e) Isolated from *Stigeoclonium helveticum;* f) Isolated from *Chlamydomonas noctigama.*

II.2 – *Pichia pastoris* as an expression system for Channelrhodopsin-2

II.2.1 – Choosing *Pichia* pastoris as the expression system for ChR2

First attempts to produce and purify ChR2 were developed using *E. coli* as the heterologous system, however, this approach was not successful [51]. The fact that, unlike BR, ChR2 was originally isolated from *Chlamydomonas reinhardtii,* an eukaryote, and successfully expressed in mammalian cells without many modifications, led researchers to try other expression systems. For example, insect (Sf9 cells)[16] and yeast (*Pichia pastoris*) expression systems have been used to produce functionally active protein. It appears that due to the eukaryotic nature of these systems, the protein acquires the correct folding, perhaps because these are phylogenetic closer to the original host of the protein than *E .coli* and therefore, capable of performing the necessary post-translation modifications, protein targeting and folding that the prokaryote is not. We chose to produce ChR2 and our variants in *Pichia* over Sf9 due to the easier manipulation of these cells and the fact that they can be grown in high-density cultures which can potentially allow for higher levels of protein expression. Moreover, expression of ChR2 has been described by different groups [33,52] using this system to accomplish goals similar to the aim in this work.

II.2.1 – The *Pichia pastoris* expression system

Pichia pastoris has been employed to produce a wide variety of recombinant proteins. This system was developed in the 70s as a source of single cell protein for animal feeding, due to its ability to metabolize methanol as its sole carbon source. Recently, *Pichia* has been used for the expression of heterologous protein.[53] In spite of not achieving the same levels of foreign protein expression as *E.coli*, *Pichia* has advantages that make it a better candidate for expression of certain proteins. Namely, being a eukaryote, *Pichia* is able to perform glycosylation, has a more suitable lipid membrane composition and thus allows for proper folding of proteins that would not acquire it in the prokaryote system[54,55]. This is especially true when it comes to membrane proteins that have a tendency to aggregate into inclusion bodies in *E. coli* but, due to the existence of eukaryotic folding/targeting machinery, can be successfully produced in P.pastoris[54]. As a result of its ability to make use of its eukaryotic machinery, Pichia provides an excellent alternative for the heterologous production of recombinant protein.

As mentioned above, *Pichia* is a methylotrophic yeast, i.e., it is able to use methanol and its sole carbon and energy source. To do so, the cell uses a specialized organelle called peroxisome, which prevents harmful chemical metabolites from damaging the cell. Inside the peroxisome there is a high concentration of an enzyme responsible for the oxidation of the alcohol (Alcohol Oxidase) into its corresponding aldehyde. When the promoter for this gene (AOX gene) was isolated it was found that it was under tight regulation, much like the classic *E.coli* lac promoter[56]. AOX gene is highly repressed by other carbon sources (glucose, ethanol, glycerol) and is only active

in the presence of methanol. This characteristic allied to the fact that it is able to generate very high levels of the enzyme under normal circumstances (5-30% of total soluble protein is AOX under MeOH induction), makes the promoter of this gene a good candidate to drive the expression of foreign proteins in the system. As such, most approaches for heterologous expression of protein in *Pichia pastoris* make use of this promoter, although others can be used (e.g. GAP promoter that results in constitutive expression by the cell[57]).

Strategies involve cloning the desired protein into an expression vector (e.g. pPICZ series) that has a homology arm to the AOX1 gene. Upon linearization of the vector and insertion into the cell, recombination events occur and the gene is inserted at the AOX1 locus (Fig.9-A). Because of the nature of this phenomena, multiple recombination events can take place and multicopy mutants can be found which usually tend to produce protein proportionally to the number of gene copies inserted into the genome[58] (Fig.9-B).

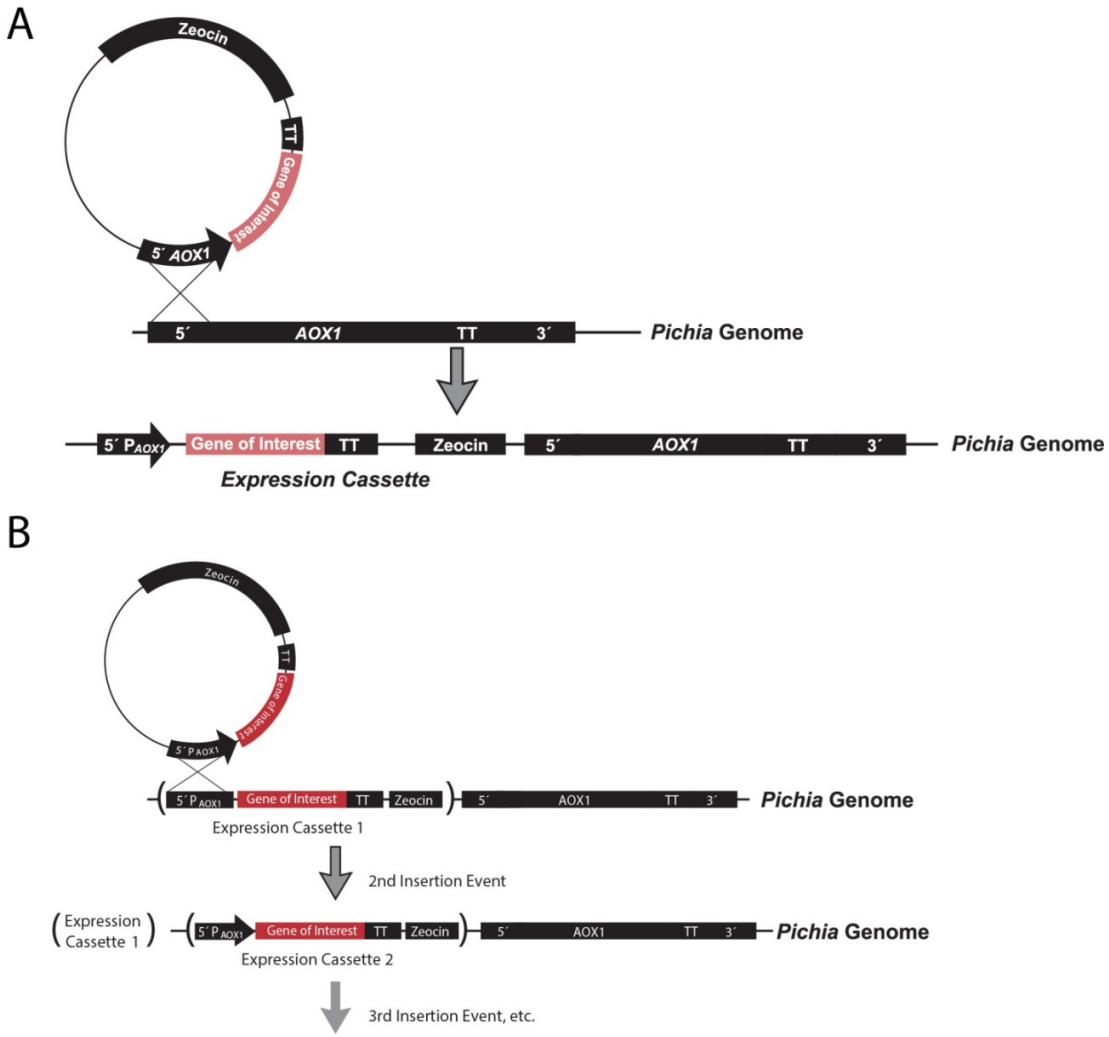

Figure 9 - Genomic integrations events in *Pichia pastoris*. A) Single copy integration: the presence of an homology arm in the vector to the AOX1 *locus* promotes, by homology recombination, the insertion of the gene of interest into the *Pichia* genome; B) multicopy integration: following the first integration, the homology sequence remains in the genome of the yeast, and subsequent events of homologous recombination, can still occur, albeit less frequent, to generate multicopy inserts of the gene of interest. Along with the gene of interest, Zeocin resistance cassette is also inserted multiple times, and is thought to confer zeocin hyperresistance to colonies.

II.3 – Time Dependent – Density Functional Theory (TD-DFT)

One can describe quantum-mechanically the electronic dynamics of a given system using the time-dependent Schrödinger's' equation (SEq). Such system may be as "simple" as a single electron or it may refer to more complex molecules (e.g. N2, benzene, amino acids, retinal, proteins…) with many electrons. However, and although the equation is perfectly known, its solution is only feasible for very small systems. One rather elegant approach to solve this problem of scalability is to use Density Functional Theory (DFT)[59]. This theory provides a simple and exact reformulation of SEq for a multiple-particle system. For the complex molecules mentioned above, DFT allows for the derivation of a set of equations that depend solely on the electron density, that is a function of the 3 space variables, instead of depending on many-body wavefunctions (in the case of SEq) that is a function of 3 variables for each electron (i.e. 3n variables where n is the number of electrons in the system).

The problem can be further simplified using what is designated as pseudo-potentials. This approach divides the atom's electrons into two groups: an inert, non-reactive group, where most of the electrons occupying lower energy levels belong; and a more dynamic group whose electrons effectively participate in interatomic interactions (higher energy/ outer electron layer). Because of these simplifications the output of the equation might be slightly different from what it is observed. However, this is not the only approximation used in DFT. The main approximation is the Kohn-Sham[60] formulation of DFT that requires the use of a non-exact form to account for the electronic correlation and to correct the kinetic energy expression. The most commonly

used approximation assumes that this term only depend on the electronic density at any given coordinates (Local Density Approximation Theory or LDA).

Due to the overwhelming amount of data processed, this equation is solved using computational methods (e.g. *octopus*, http://www.tddft.org/programs/octopus/wiki/index.php/Main_Page [61,62,63]). As a first step, an approximated value of the solution expected from the algorithm is given, usually based Linear Combination of Atomic Orbitals theory (LCAO). After having this first solution the program solves the equation using self-consistent iteration cycles. This method generates a 3D function of the electron density of the molecule at its ground state and we can be used for Time-dependent DFT.

At this stage, the simulation of the electronic cloud of the molecule is given a stimulus and is studied how it evolves during a given time window. In our case, we are interested in the effect of light of the visible spectra on the molecule, and thus a very fast "flash of light" (10^{-17} seconds). As this stimulus is so fast, a Fourier transformation (FT) will evidence that we are exciting the molecule, at the same time, with electromagnetic radiation with a very wide spectrum of frequencies. This stimulus is commonly known as a "kick". The kick must be applied across the 3 different axis and later compiled into a final effect. After each kick the system evolves and changes its dipole moment. If the kick is not too strong we can use the approximation that a FT of the change of dipole moment of the molecule is actually the absorbance of the molecule to the various wavelengths. In order to obtain a "perfect" spectrum we would have to keep propagating the equation to infinitum. Moreover, this system does not account for energy transfers between adjacent molecules that may occur in nature; hence we limit

our time-propagation to about 10000 time-steps. After these runs we should have as output of several values of absorbance as a function of wavelength which provides the a simulated absorbance spectra of the molecule studied. This system may then be adapted to predict the effect of discrete mutations, that by changing the electron density cloud in the simulation, produce a new hypothetical absorbance for the molecule understudy. This method has proven to be very accurate in describing biological chromophores, such as fluorescent proteins, the Genji-Botaru luciferin, and other biological systems (flavins, porphyrins, DNA).[64–66]

Chapter III – Materials and methods

Materials and methods

III.1 - Materials

III.1.1 – Organisms

Table 2 – Organisms used in the present work, their experimental use and source.

Organism	Experimental use	Source
Escherichia coli DH5α	Molecular cloning and plasmid amplification	Invitrogen
Pichia pastoris (X-33 strain)	Protein expression and purification	Invitrogen
Pichia pastoris (SMD1168H strain)	Protein expression and purification	Invitrogen
HEK293T	Imaging experiments / Electrophysiology experiments	CNC, Coimbra, Portugal
Primary Rat Cortex Neurons	Electrophysiology experiments	Primary Cultures

III.1.2 – Vectors

All vectors used in this study were subjected to digestion analysis and partial sequencing to confirm accurate cloning procedures.

Table 3 – DNA vectors used in the present study, their relevant features and source.

Vector Designation	Relevant features	Source
pcDNA3.1-hChR2	CMV promoter; hChR2-eYFP; AmpR	addgene.org (K. Deisseroth)
pPICZ A	AOX1 promoter; c-myc tag; 6x His Tag; ZeoR	Invitrogen

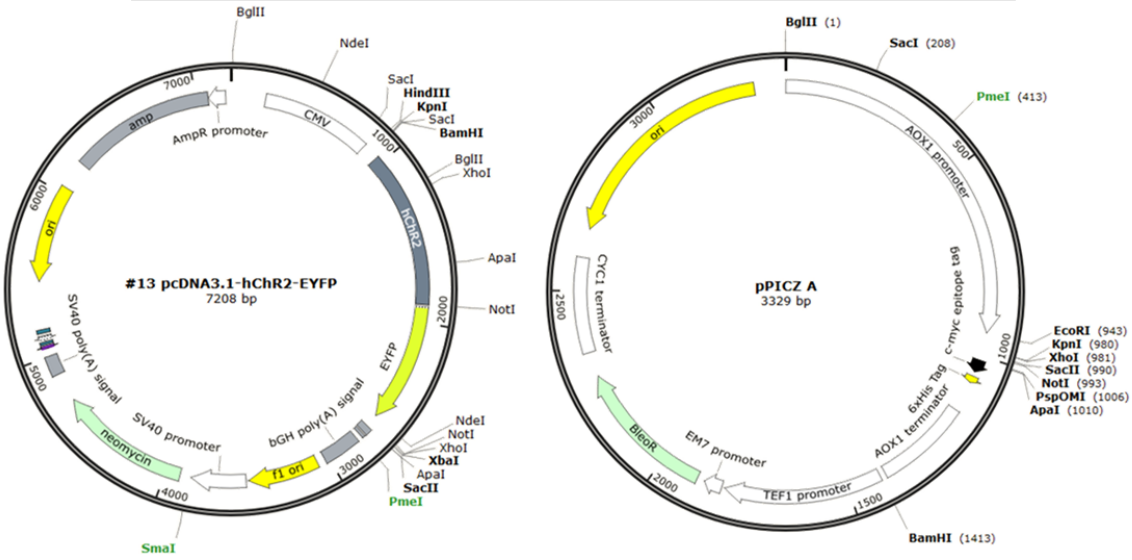

Fig 10- Vectors used in the present study. pcDNA 3.1, provided by Karl Deisseroth, encodes a fusion protein of ChR2 and eYFP under the control of a ubiquitous mammalian promoter (CMV). pPICZ A, acquired from Invitrogen, has the specific promoter for expression in *P. pastoris* (AOX1) and the resistant to Zeocin necessary for selection of positive clones. Both vectors show the relevant restriction sites.

III.1.3 – Primers

All primers used in these studies (Table 4) were purchased from Stabvida (Setúbal, Portugal)

Table 4 – Primers used in the study and their respective experimental use.

Primer	Sequence (5'➔3')	Experimental use
MutScr_1_F	GAGAACCATGGGACTCCTTGTC	Mutation Screening
MutScr_1_R	CATACCCCAGCTCACGAAAAAC	Mutation Screening
L221D_F	GTCATCTTCTTTTGTCTTGGAGATTGCTATGGCGCGAACACATTTTTTC	Directed site mutagenesis
L221D_R	GAAAAAATGTGTTCGCGCCATAGCAATCTCCAAGACAAAAGAAGATGAC	Directed site mutagenesis
F217D_F	CGGCTATGTTAAAGTCATCTTCGACTGTCTTGGATTGTGCTATGGC	Directed site mutagenesis
F217D_R	GCCATAGCACAATCCAAGACAGTCGAAGATGACTTTAACATAGCCG	Directed site mutagenesis
yChR2_F	GCCGAATTCAAAAATGTCTGACTATGGCGGCGCTTTGTC	yChR2 fragment
yChR2_R	GCCGGTACCGGCGGCCGCTGGCACG	yChR2 fragment
AOX1_F	GACTGGTTCCAATTGACAAGC	pPICZ A Screening
AOX1_R	GCAAATGGCATTCTGACATCC	pPICZ A Screening

III.2 – Methods

III.2.1 – ChR2 absorption spectra theoretical predictions

Theoretical predictions of ChR2 wild-type and mutant's absorption spectra were generated by Center for Computational Physics at the University of Coimbra using Octopus software[61–63] (http://www.tddft.org/programs/octopus/wiki/index.php/Main_Page). Residues to be mutated were based on several considerations. First, because the function of the channel has to remain intact, residues in the ion pore transmembrane sequences were discarded. Second, when mutating the residues, one must consider that change of charge/polarization results into greater effects than substituting for a similar amino acid (e.g. glutamate by aspartate that share a similar chemical characteristics). Finally, the choice of residues was also based on information regarding the polarization of the retinal molecule provided by the Center for Computational Physics.

Molecular graphics and analysis were performed using PyMOL (The PyMOL Molecular Graphics System, Version 1.5.0.4 Schrödinger, LLC.) and UCSF Chimera (University of California, San Francisco)

III.2.2 – Molecular Biology

Preparation of competent bacteria and transformation

Using E. coli DH5α strain, competent bacteria were prepared using standard protocols. Briefly, after inoculation of 150mL of LB media, cells were allowed to grow at 37°C until OD_{600}=0,4 was reached. From here on all steps were performed in an ice slurry. Cells were pelleted at 3000 xg for 10min at 4°C and the media carefully removed. The pellet was carefully resuspended in 20mL of cold 0.1M CaCl2 and incubated for 30min. The suspension was centrifuged at 3000 xg for 10min and finally resuspended in 3mL of 0.1M CaCl2 + 15% Glycerol, aliquoted, frozen in a dry ice/ ethanol slurry and stored at -80°C until transformation. To perform the transformation protocol, an aliquot was thawed on ice and plasmid DNA (100ng-1ug) was mixed with the cells and the solution was allowed to rest for 30min on ice. Afterwards a heat shock step was performed at 42°C for 45 seconds and returned to ice for another 5min. After addition of 9 volumes of LB cells were incubated at 37°C for 1hour, after which there were plated in LB/Agar plates containing the appropriate antibiotic.

Generation of hChR2 mutants

Before the generation of the mutants, a restriction analysis using the DNA from original glycerol stock containing pcDNA3.1-hChR2 (Plasmid 20939: pcDNA3.1/hChR2-EYFP from addgene.org) was performed using XbaI (New England Biolab, NEB) and BamHI (NEB). After the digestion, the product was loaded together with DNA Loading Buffer (0,25% Bromophenol Blue; 40% Sucrose) into a 1% agarose gel and separated,

until obtain good enough band resolution was obtained, in TAE buffer (40mM Tris Acetate; 1mM EDTA). Bands were visualized under UV light. hChR2 mutants were generated using a directed mutagenesis strategy. Briefly, synthesized primers (Stabvida) (Table 4) were designed, using the PrimerX algorithm (http://www.bioinformatics.org/primerx/), to hybridize with part of the original hChR2 except for the nucleotides targeted for mutation. The PCR reaction was performed as follows: 1uL of PrimeSTAR HS DNA Polymerase (2,5U/uL);10uL 5x PrimeSTAR Buffer; 200nM of each primer; 200nM of an equimolar dNTP mix; 500ng of pcDNA3.1-hChR2 and ddH2O up to 50uL with temperatures of 92°C, 30sec; 18 cycles of: 95°C, 30sec; 55°C, 30sec; 68°C, 510sec. All PCR products resulting from these reactions were incubated with DpnI and screened in 1% agarose gel. 20uL of the DpnI treated DNA was used to transform competent bacteria which were then plated onto LB/Agar (amp+) plates. DNA from the selected transformants was extracted using a mini-prep kit (NZYtech) and sequenced for the presence of desired mutation with SCRRev and SCRFw primers (Stabvida).

hChR2 cloning into pPICZ

hChR2 sequence was cloned into pPICZ A vector (Invitrogen) in frame with 6xHis Tag. A set of primers was designed to add a 5' EcoRI and 3' KpnI restriction sites to the hChR2 fragment. Additionally, a yeast Kozac Sequence (AAAAATGTCTG) was added to the 5' to further increase expression[67]. This final, amplified, fragment was

named yChR2. The PCR reaction was performed as it follows: 1uL of PrimeSTAR HS DNA Polymerase (Takara) (2,5U/uL);10uL 5x PrimeSTAR Buffer; 200nM of each primer; 200nM of an equimolar dNTP mix; 300ng of pcDNA3.1-hChR2 and ddH2O up to 50uL with temperatures of 98°C, 30sec; 35 cycles of: 98°C, 10sec; 55°C, 10sec; 72°C, 120sec and an additional 5min at 72°C. After confirming amplification, the DNA sample was treated with 1uL of Proteinase K (NEB) for 30min at 55°C, purified with DNA Clean & Concentrator (Zymoresearch) and digested with KpnI (NEB) and EcoRI (NEB). After 3 hours of digestion, all the material was loaded into a 1% agarose gel and, after excision of the desired band, purified with Gel DNA Recovery Kit (Zymoresearch). In order to obtain the acceptor fragment from pPICZA, the latter was digested using the same reaction as yChR2 followed by incubation with CIP (NEB) to prevent vector re-circularization. After purifying pPICZ A, the ligation protocol was performed in a total volume of 10uL using T4 Ligase (NZYtech) according to manufacturer's instructions. After ligation, the full reaction volume was transformed into DH5α and colonies were selected in 25ug/ml Zeocin (Invitrogen) LB/Agar plates. Positive colonies were screened with PCR reaction using AOX1fw and AOX1rev primers and finally sent to sequencing to confirm the insertion of yChR2 and the frame it occupied.

Vector linearization

Because electroporation in yeast is more efficient when the genetic material is linearized, pPICZ A – yChR2 was digested to yield a linear fragment. Briefly, 10ug of

DNA were digested with 5uL of CutSmart Buffer, 2uL of PmeI (NEB) in a final volume of 50uL for 3 hours. After three hours, another 1uL of enzyme was added and the digestion continued for another 2 hours after which linearization was confirmed in agarose gel. The product was then purified using DNA Clean & Concentrator (Zymo Research).

Pichia pastoris electroporation

Two days before electroporation, a pre-inocule of 5mL of YPD media was inoculated with a single *Pichia pastoris* colony and let to grow overnight in a 50mL conical tube at 30°C. On the next day, 500mL of YPD were inoculated with 0.1-0.5 mL of the pre-inocule prepared the day before and grown overnight to a final OD600=1.3-1.5. After obtaining the optimal OD, cells were harvested by centrifugation at 1500 xg for 5min at 4°C. After this step the cells were washed twice with sterile water (500mL and 250ml respectively), washed once in 20 mL of 1M Sorbitol (sigma) and finally resuspended in 1mL of 1M Sorbitol (all centrifugations were conducted at 1500k xg for 5min at 4°C). To perform the electroporation, 80uL of cell suspension were mixed with 20uL of linearized DNA (5-10ug) and pulsed using MicroPulser™ Electroporator's "Pic" protocol (BioRad). After the pulse, cells were incubated on ice for 5min after which 1mL of 1M Sorbitol was added to the cuvette and cells were grown for 2hours at 30°C, without agitation. Finally, cells were plated onto YPD plates with 1000ug/ml, 100ug/ml and no Zeocin.

III.2.3 – yChR2 expression and purification from *Pichia pastoris*

Protein expression and extraction

Single colonies were picked from 1000ug/ml plates (hyperesistant clones) and re-streaked onto 1000ug/ml zeocin YPD plates to yield isolated colonies. To assess the expression of clones, a small scale induction was performed. Briefly, colonies were allowed to grow in 5mL of YPD o.n. supplemented with Zeocin. The next day, glycerol stocks of the clones were obtained by diluting 800uL of culture into 500uL of 50% glycerol. 100uL of the culture was then added to 5mL of BMGY (1% yeast extract, 2% peptone, 100mM potassium phosphate, pH 6, 1.45% YNB, $4x10^{-5}$ % biotin; 1% glycerol) and grew o.n.. This pre-inocule was then used to start a 50mL BMGY culture until 4-6 OD600 was achieved. Finally, to induce expression of the protein, the cells were pelleted and ressuspended into BMMY (1% yeast extract, 2% peptone, 100mM potassium phosphate, pH 6, 1.45% YNB, $4x10^{-5}$ % biotin; 2.5% MeOH and 10uM retinal) to a final OD of 1 and incubated for 24-30hours. After induction cells were harvested by centrifugation at 3000 xg for 10min. To yield higher amount of starting material, the protocol described previously was upscaled as required, most frequently to a final volume of 500mL of BMMY.

Using the cell pellets previously obtained, homogenization buffer (Homogenization buffer – 11,3mM NaH2PO4 (Acros); 100mM NaCl (Acros); 1mM EDTA (Fisher); 5% glycerol (Fisher); 1mM PMSF; cOmplete ULTRA Tablets, Mini EDTA-free, EASYpack (Roche)) was added in a proportion of 15mL to 500mL of starting culture. To achieve cell lysis (unless otherwise specified) a French Press system was used (Thermo). Cells

were passed through the French press a minimum of 4 times at ~7000 psi. In order to remove the unbroken cells and other unwanted cell debris, the sample was centrifuged at 8000 xg for 20 min and the pellet was discarded. To obtain the enriched membrane fraction, the supernatant was centrifuged at 180 000 xg for 1 hour, resuspended in solubilization buffer A (20mM Potassium Phosphate pH 7,4 (acros); 200mM NaCl; 5% Glycerol; 1% (m/v) n-Dodecyl β-D-maltoside (calbiochem); 250mM L-Arginine (sigma); 3uM retinal (sigma); 10mM imidazole (sigma); 0,1mM PMSF (Acros)) in a ratio of 5mL/500mL of starting culture. Membrane fraction was then solubilized overnight and insolubilized membrane fraction was removed by ultracentrifugation at 180 000 xg for 1 hour.

Nickel chromatography

The previously obtained solubilized fraction was diluted 1:10 in buffer B (Solubilization buffer B - 20mM Potassium Phosphate pH 7,4; 200mM NaCl; 5% Glycerol; 0,03% (m/v) n-Dodecyl β-D-maltoside; 0,1mM PMSF, 10mM Imidazole) to decrease the concentration of protein and concentration of DDM to values compatible with the nickel column being used (1ml HisTrap FF Crude, GE Healthcare). Before loading the column with the protein extract, 10-15 volumes of solubilization buffer B (10mM imidazole) were used to equilibrate the column, by means of a peristaltic pump (~0.7ml/min). The protein extract was loaded using the same system and a sample was collected as flowthrough. 10 volumes of buffer B were used to re-equilibrate the column after which it was inserted into an AKTA FPLC system where OD260 was monitored.

The system was set to a flow rate of 0.7ml/min and equilibrated with buffer B until a stable baseline (OD260) was achieved. To wash the column buffer B with 25mM was used and subsequently increased to 100mM, 250mM and 500mM imidazole. Throughout the process fractions of 1.7ml were collected.

Sample dialysis and concentration

Samples were dialyzed and concentrated using Amicon® Ultra-15 Centrifugal Filter Units 10kDa (Millipore) according to manufacturer's instructions. Full volume of the dialysis unit was replaced 5x times after which it was concentrated to about 500uL.

Protein quantification

Protein quantification was performed using Pierce™ BCA Protein Assay Kit (Thermo) according to manufacturer's instructions and using the supplied 2mg/ml BSA standard.

Gel electrophoresis and Western blot

The separation of denatured proteins was accomplished using SDS-PAGE with a 12% acrylamide for resolving and 4% stacking (Table 5) and ran in 1x Running buffer

(5x Running buffer – 15g of Tris base (Fisher); 72g of glycine (Fisher) and 5g SDS (Fisher)) at 50-90V. Samples were diluted into 4x Laemmli buffer (Biorad).

Table 5 – SDS-PAGE gel composition

Gel percentage	Reagent	Volume (for 4 gels)
12%	dH_2O	12,2 ml
	1.5M Tris pH 8,8 (Fisher)	11,5 ml
	40% acrylamide (Fisher)	10,6 ml
	20% SDS (Fisher)	350 ul
	10% AMPS (Acros)	480 ul
	TEMED (NZYtech)	70ul
4%	dH_2O	9,5 ml
	0,625M Tris pH 6,5 (Fisher)	3,8 ml
	40% acrylamide (Fisher)	1,5 ml
	20% SDS (Fisher)	150 ul
	10% AMPS (Acros)	225 ul
	TEMED (NZYtech)	30 ul

For western blot analysis, proteins were transferred onto a PVDF membrane (GE Healthcare, Lifesciences) by electroblotting (100 V, 2 hours, 4°C). The membranes

were washed in Tris-buffered saline (137 mM NaCl, 20 mM Tris-HCl, pH 7.6) containing 0.1% (v/v) Tween-20 (TBS-T), and blocked in TBS-T with 5% (w/v) low-fat milk. Membranes were probed with His-Tag antibody (Cell signaling) overnight in TBS-T with 5% BSA at 4°C. Membranes were thoroughly washed in TBS-T and incubated at room temperature for 3 hours with the secondary anti-rabbit antibody (Jackson Laboratories). After washing the membranes again, incubation with ECL 2 reagent (Pierce) according to manufacturer's instructions was performed. Membranes were scanned with the Storm 860 scanner (Amersham Biosciences) .

Coomassie protein staining

Gels were incubated with staining solution (0.05% Coomassie Brilliant Blue R-250 (Fisher), 25% methanol (Fisher) and 5% acetic acid (Fisher)) for 10-15min. The gel was then washed in destaining solution (25% methanol; 5% Acetic acid) once for 1 hour and then overnight.

Silver protein staining

For the silver staining protocol, gels were incubated according to Table 6:

Table 6 – Silver protein staining protocol used.

Solution	Time
25% MeOH; 5% HAc (Fisher)	30min
50% EtOH	10min
30%EtOH	10min
0,2g/L Sodium thiosulfate (Acros)	1min
dH_2O	2x 20min
2 g/L Silver Nitrate (Acros)	20min
dH20	1min
30g/L Sodium Carbonate (Acros); 10mg/L Sodium thiosulfate, 0,02% formalin	Up to 20min
50g/L Tris, 2,5% HAc	1min to stop the reaction

III.2.4 – ChR2 absorption spectra determination from HEK293T cells

HEK293T were maintained in DMEM with 10% heat-inactivated fetal bovine serum (FBS) supplemented with Penicillin-Streptomycin and kept at 37°C in a humidified incubator with 5% CO_2/95% air. 24 hours prior to transfection, cells were plated at a density of 500 000 cells / well in 6 multi well plates coated with poly-L-lysine.

Cells were transfected using Lipofectamine (Invitrogen) LTX according to manufacturer's instructions with pcDNA3.1-ChR2-eYFP plasmid. After 48 hours of expression, cells were washed twice with saline solution, trypsinized (0.25%) and resuspended in saline solution. After resuspension, measurements of the absorption spectra were performed.

III.2.5 – ChR2 membrane trafficking experiments

HEK293T were maintained in DMEM with 10% heat-inactivated fetal bovine serum (FBS) supplemented with pen-strep and kept at 37°C in a humidified incubator with 5% CO_2/95% air. For imaging studies, the cells were plated at a density of 13,000 cells/cm-2 in glass coverslips. 24 hours after plating, the cells were transfected, using Lipofectamine LTX (Invitrogen) according to manufacturer's instructions, with the plasmids coding the ChR2 mutants fused with eYFP flurophore. Cells were allowed to express the protein for 24 hours after which they were washed in PBS at least three times, stained with Hoescht and fixed in 4% paraformaldehyde and. All images were obtained with confocal microscopy using Zeiss LSM 510 Meta microscope.

III.2.5 – Electrophysiology experiments

HEK293T electrophysiology

HEK cells were maintained as described for imaging studies. Cells were plated onto 15mm coverslips at a density of approximately 100,000 cells / coverslip. On the following day cells were transfected with ChR2 plasmids using lipofectamine LTX according to manufacturer's instructions. Cells were allowed to express ChR2 for 24hours, supplemented with 3uM of all-*trans* retinal to a maximum of 72hours. Coverslips were mounted onto a microscope stage coupled with the electrophysiology equipment and bathed with an external solution consisting of (in mM): 140 NaCl; 2 $MgCl_2$; 2 $CaCl_2$; 2 KCl; 10 HEPES (pH 7.2 with CsOH and 300~320 mOsm with glucose). Pipettes were pulled using a P-87 micropipette puller (Sutter) from borosilicate glass with a final resistance of 2-6MΩ and filled with (in mM) 110 NaCl; 5 EGTA; 2 $MgCl_2$; 1 $CaCl_2$; 5 KCl, 10 HEPES (pH 7.2 with CsOH and 290-310 mOsm with glucose). Recordings were made using Axopatch 200A amplifier (Axon CNS, molecular devices) and sampled with Clampex digidata 1200 (Axon CNS).

Primary cortical neurons electrophysiology

Primary cultures of rat cortical neurons were prepared from the cortices of E18-E19 Wistar rat embryos. Briefly, cortices where washed in ice-cold HBSS three and five

times, prior and after trypsin treatment, respectively. Cells were mechanically dissociated, no more than 10-15 times with HBSS. After counting, cells were centrifuged at 800 xg for 5min and resuspended to the desired final concentration (usually 1.5 to 5 million cells / 100uL) in IngenioTM Electroporation Solution (Mirus Bio LLC, Madison, WI). 100uL of the resuspension electroporated using the AMAXA system (Lonza) together with 2-5ug of DNA). After the electroporation protocol, cells were seeded onto 2 coverslips (15mm) coated with poly-D-lysine and MEM supplemented with 10%FBS. After 4hours, the media was replaced with Neurobasal medium (Gibco) supplemented with 2% NeuroCult SM1 and 0.5mM glutamine and maintained inside an incubator at 37°C in a humidified atmosphere with 5%CO2/95% air. For the electrophysiology experiments, the same equipment as for the HEK293T cells was used. We used the same external solution as for HEK293T cells whereas internal solution was replaced with: (in mM) CsF 35 , CsCl 100, EGTA 10, HEPES 10, and pH 7.32 (with CsOH).

Chapter IV – Results and discussion

Results and discussion

IV.1 – Theoretical selection of target residues to be replaced in ChR2

As a result of the collaboration between our laboratory and the group of Computational Physics from the physics department in University of Coimbra, two mutations were selected for further analysis in this work. These were F217D and L221D mutations (numbering according to the structure 3ug9 deposited in http://www.rcsb.org/pdb published by [16]) since this was the structure used for the computational calculations using the Octopus algorithm . These mutations translate to F179D and L183D, respectively, when considering the "wild-type" ChR2 sequence presented in Fig. 3. The predicted spectra are presented in Fig. 11. As seen in Fig.12-a these residues are located near the retinal pocket and are located far from the hydrophobic ion pore, which is thought to be important in order to preserve the gating proprieties of the rhodopsin. In order to produce as a great effect on the absorption spectra as possible, the charge of these residues was changed. Both Leucine (L) and Phenylalanine (F) have no charge in their side-chains at physiological pH and are highly hydrophobic due to their non-polar nature Fig.12-b [68]. As a result, both amino acids were mutated to Aspartate (D) residues, since this presents a negative charge a physiological pH which will theoretically lead to a change in the electrostatic environment of the retinal molecule. Other simulations using the same residues as targets but replacing for a positive amino acid (e.g. histidine) are predicted to result into a blue-shift rather than a red-shift effect on the opsin absorption spectra (data not

shown). This information might prove useful to apply to other molecules or even to obtain a pair of ChR2 that have non-overlapping absorption spectrum.

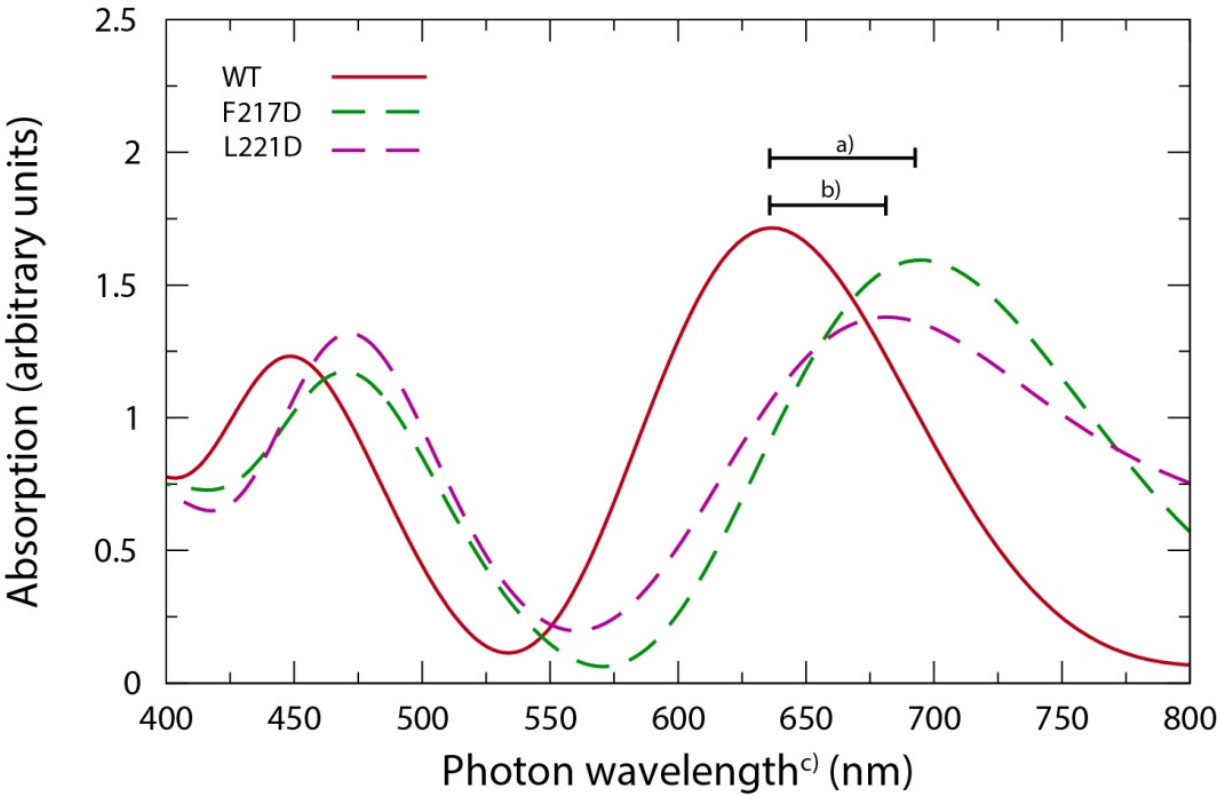

Figure 11 - Theoretical predictions of the opsins' absorption spectra obtained from Octopus algorithm. a) and b) depict the red-shifts between WT/F217D and WT/L221D, respectively. a) = 60nm; b) = 45nm. Note c): wavelength output form TD-DFT analysis is systematically right-shifted, e.g. the experimental absorption peak at pH 6.0 of dark adapted Wt ChR2 is centered at 480nm. These results are from Micael J.T. Oliveira, Bruce F. Milne and Fernando M.S. Nogueira (unpublished data).

Albeit designed as single mutations it is possible to use both modifications and attempt to generate a double mutant with a potential senergistic effect between them as previously described for other channel proprieties (e.g. SSFOs). As a result, even if only small shifts result from single mutations it is possible that by combining several modifications one can achieve a greater shift.

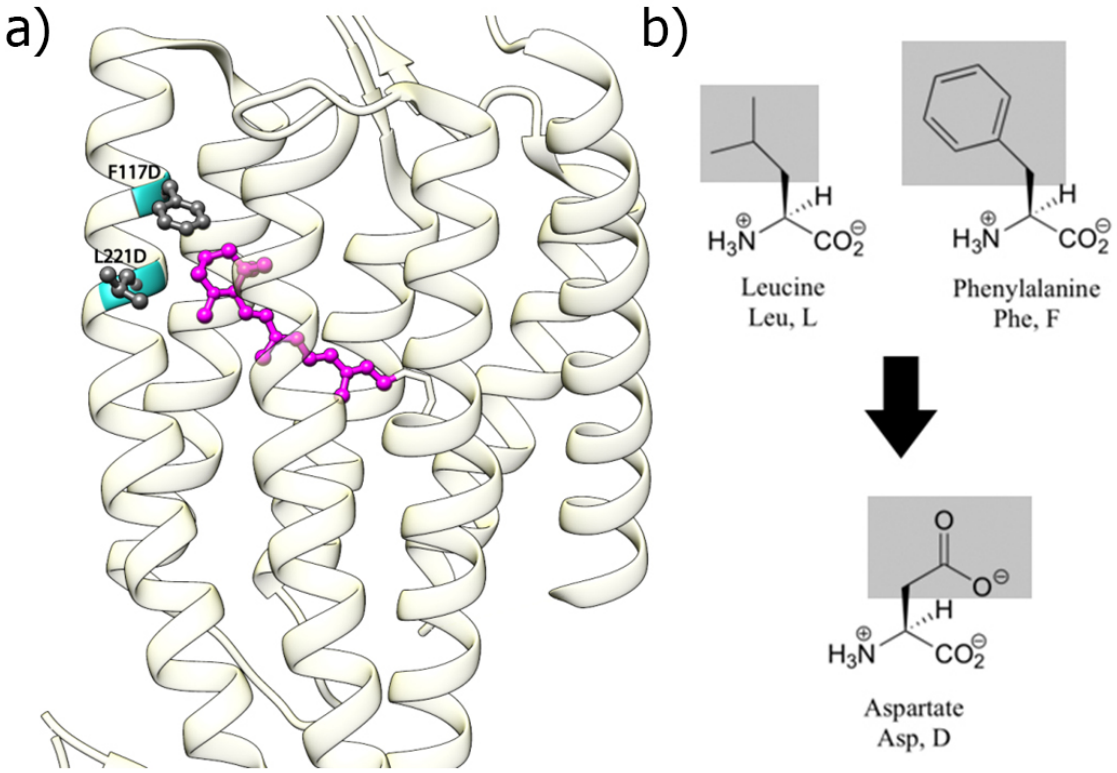

Figure 12 - Candidate residues for mutation in this study. Pink : Retinal; Blue and Black: Selected residues based on C1C2 structure[16]; Structures of the amino acids replaced in ChR2 : Phenylalanine(179) and Leucine(183) for Aspartate. Grey highlights sidechains of the amino acids at physiological pH.

IV.2 – Generation of ChR2 mutants and cloning into pPICZ-A vector

In order to test the viability of the suggested modifications to the ChR2 primary structure, directed site mutagenesis was performed. To generate the mentioned modifications, the vector pcDNA3.1-hChR2 was used. However, as this is not an appropriate heterologous expression vector in the *Pichia pastoris* system, the sequence of ChR2 was shuttled to a pPICZ series expression vector, after confirming the modified bases (Fig.13).

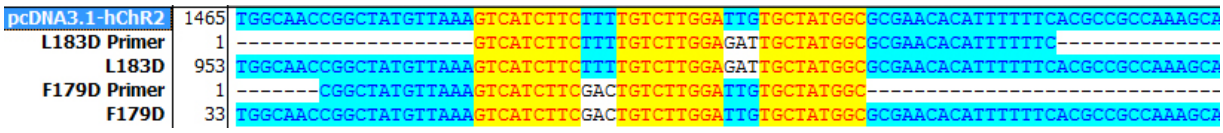

Figure 13 – Sequencing of pcDNA3.1-hChR2 after directed site mutagenesis protocol (forward primers shown in the figure) using the MutScr_1_F primer confirming the successful mutation.

After confirming the mutations, primers to amplify ChR2 were designed and, to improve the expression in yeast, a Kozac sequence was added along with two new restriction sites (Fig.14). After digesting both the insert and the pPICZ vector with EcoRI and KpnI, ligation was performed and the colonies were screened for the insertion of the yChR2 fragment using primers that flank the region of insertion of the cloned fragment: AOX1F and AOX1R (Fig.15-a). The positive colonies were chosen based on the weight of the bands and a single colony was sequenced to confirm the insertion of the fragment in frame with the Histidine tag from pPICZ-A as well as the presence of the previously

generated mutation. Although the results shown are from experiments using WT-ChR2, these are also representative of the mutations since the same rational was applied.

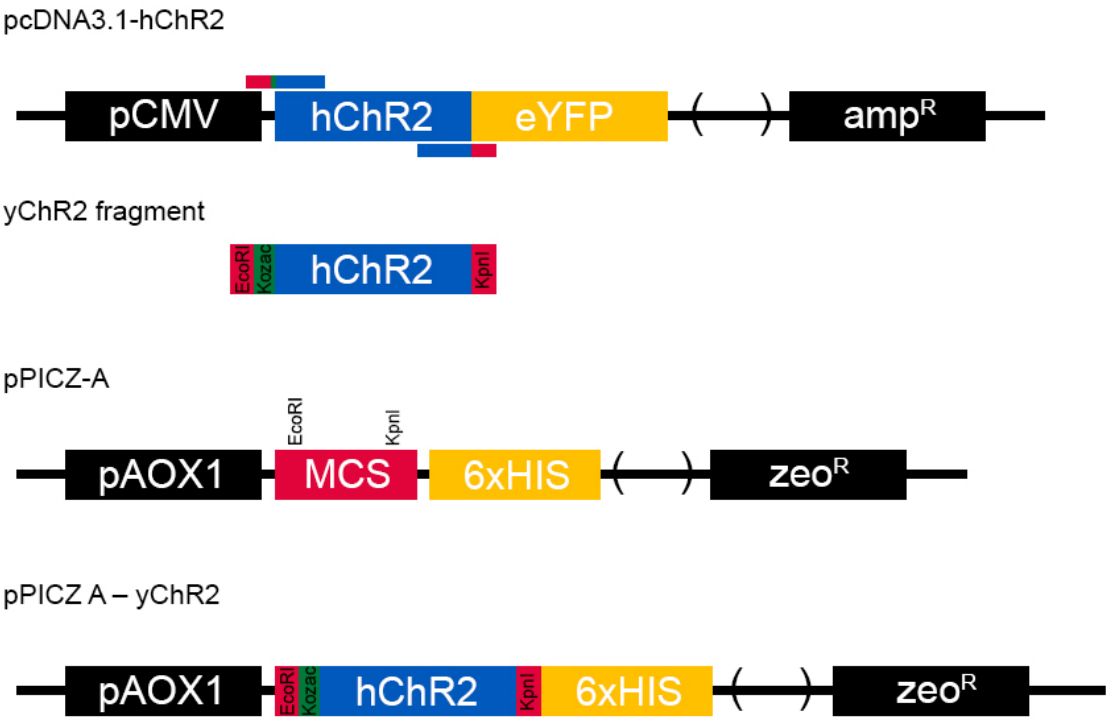

Figure 14 – Cloning strategy used to shuttle ChR2 from pcDNA3.1 vector to pPICZ A. Pink : restriction sites; Green : Kozac sequence; Yellow: hexa-histidine tag; Black : other relevant features

Finally, because integration events occur with a higher probability with a linearized vector rather than a circular one[69], pPICZ A – yChR2 was digested with PmeI enzyme that has a single cutting site in the AOX1 promoter. To confirm the linearization of the vector and due to the high amount of DNA material used, gel electrophoresis was used to determine the necessary time to linearize the genetic material (Fig.15-b). As

depicted in the figure, the 5 hour incubation yielded the highest amount of cut DNA (~4200bps), as such this was the incubation time used.

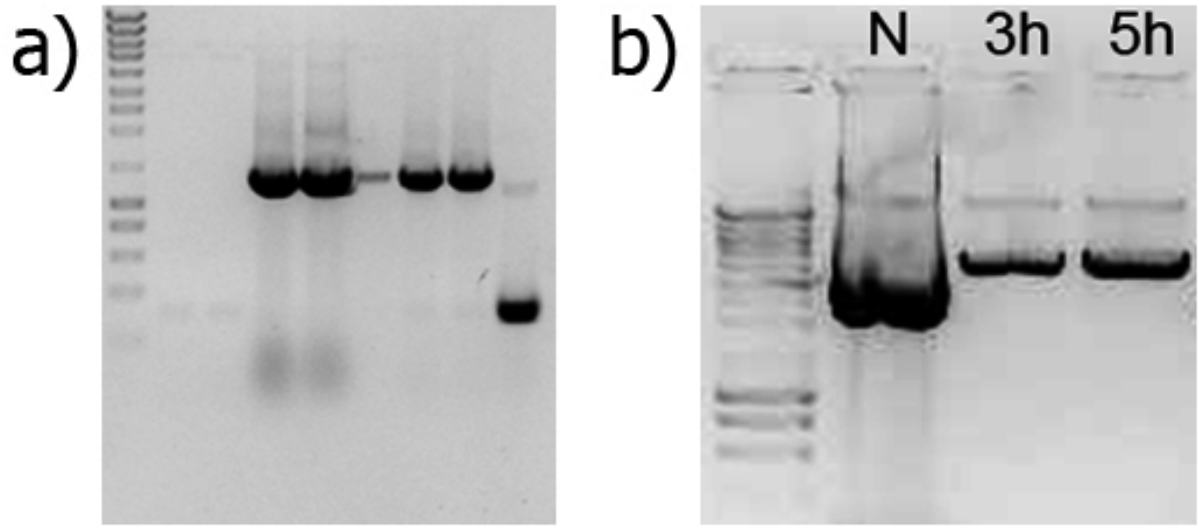

Figure 15 – a) Confirmation of the insertion of yChR2-WT in pPICZ vector by PCR screening. Positive bands corresponding to the size of an amplified fragment of yChR2 (~900bps) plus pPICZ vector (~350bps) in the lanes 1 through 4 and a negative band corresponding to the sequence of pPICZ alone (~350) in lane 5. **b) pPICZ A – yChR2 linearization with PmeI restriction enzyme.** N- Negative control; 3h, 5h – 3 and 5 hours of digestion, respectively.

IV.3 – ChR2 expression in *Pichia pastoris*

Previous attempts to isolate Channelrhodopsin-2 from *P. pastoris* have been successful[34,40,52,70–73]. These experiments, although developed by different groups, share, to some degree, common methodologies. Hence, we tried to base our experiments using previously established protocols.

Selected X33 strain colonies were chosen based on their growth in high Zeocin concentration in YPD plates (1000ug/ml) which, as mentioned above, usually correlate with higher levels of protein expression. These plates presented a two orders of magnitude decrease in the number of colonies relative to the 100ug/ml plates.

ChR2 expression was induced at an O.D. 1 for 24-30hours in BMMY (2.5% MeOH) media supplemented with retinal[71]. First studies to confirm the expression of ChR2 protein revealed a high tendency of the protein to aggregation (Fig.16) which is not surprising due to the membrane nature of the protein[74] as well as several observations that opsins have a high tendency to aggregate in eukaryotic systems[17,50,52].

Although it is clear that in the presence of ChR2 DNA and MeOH induction there is signal in the western blot, it is impossible to confirm the size of the protein which was theoretically calculated to be 38kDa (http://web.expasy.org/compute_pi/). After several experiments we concluded that the original sample had to be diluted before loading onto the gel in order to see the apparent weight of the protein (Fig.17). This finding could be explained by the fact that ChR2 is aggregation prone, and therefor stabilizing agents are needed to solubilize it. Thus, when we increase the ratio of homogenization buffer to

protein, protein-protein interactions will decrease and interactions between the buffer and protein will increase leading to less aggregation, hence more solubility.

Interestingly, when expressing in *Pichia pastoris,* ChR2 appears as two distinct bands at similar weights which probably correspond to a glycosylated and non-glycosylated form of the protein, as shown by O. Ernest *et al* using VChR[75]*,* by digesting the protein with PNGase F, an enzyme that removes the most common glycosylations performed by the yeast, collapses the two bands to a single band.

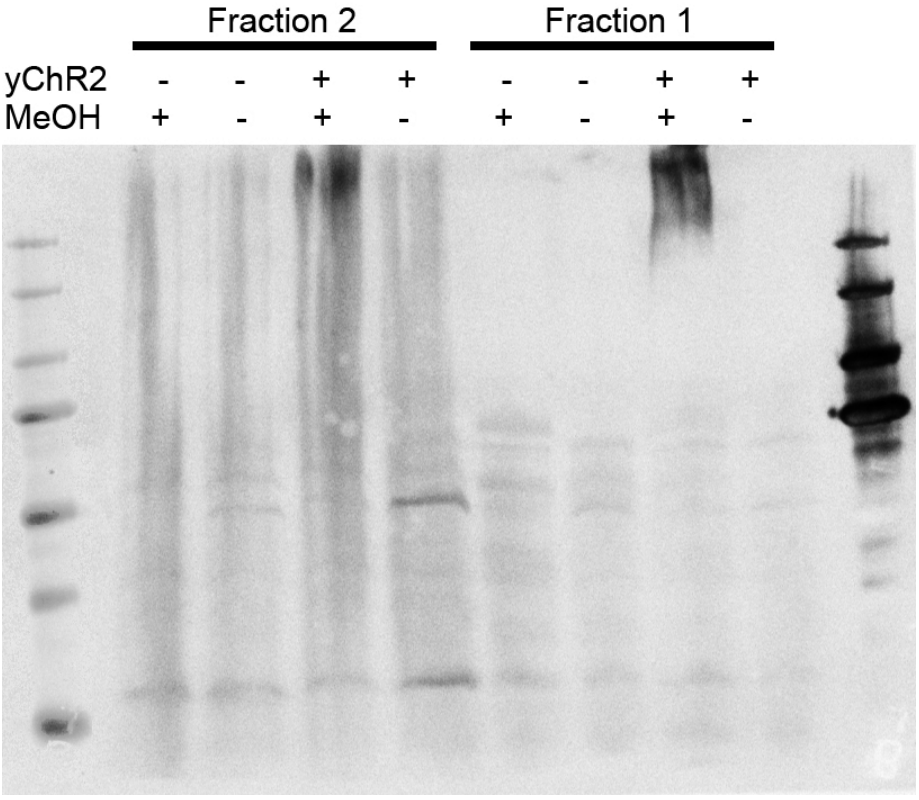

Figure 16 – Control of ChR2 expression in *Pichia pastoris*. After lysis, the cell extract was submitted to centrifugation, fractions 1 and 2 represent the supernant and pellet of this process, respectively.

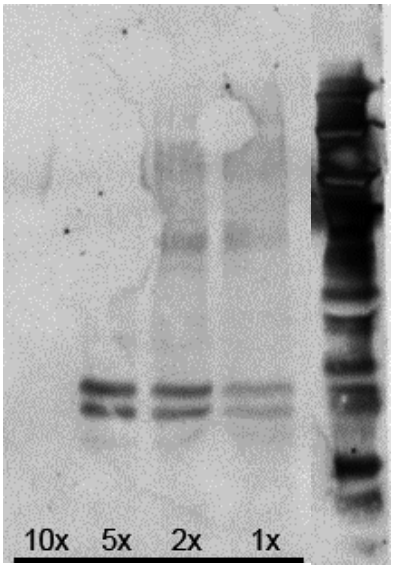

Figure 27 – Migration profile of ChR2 produced in Pichia pastoris. Optimization of conditions to observe the apparent weight of ChR2. 1x, 2x 5x and 10x represent the dilution made with homogenization buffer. 250ug of protein were loaded in the 1x well.

IV.4 – Lysis methods comparison

In an attempt to determine the best method to achieve cell lysis of *Pichia pastoris,* small scale induction of ChR2-WT production was performed and several methods tested in parallel. Their inherent robustness, attributed to high contents of branched glycan chains, chitin and glycoproteins[76], results into difficulties to extract protein without specialized methods and equipment. After reviewing the literature we selected four methods that were possible to use in our laboratory.

Glass bead extraction works by vigorously vortexing the sample with small acid washed glass beads breaking the cell membranes and releasing their contents. Comparing to other methods, glass bead extraction requires no special apparatus if done in a small scale. Unfortunately the method becomes challenging when it comes to volume scalability and, without the specialized equipment (Bead-beater), did not produce a particular high yield in our hands.

Sonication equipment which is used in the breaking of *E.coli* cells [77] was also applied to our yeast cultures. This method is fast and easy to use, however it is particularly difficult to scale to bigger volumes (>5ml). Additionally, longer protocols may result in overheating of the protein sample potentially leading to protein degradation.

Pressure systems (e.g. French Press system), lyse cells by creating large differences in pressure (ideally between 7000-20000 PSI) that result in cell wall bursting. In spite of requiring specialized and expensive equipment, this process presents very high yields, little time consumption and opportunity to use considerable sample amounts at a time (>20mL).

Lastly, we used a propriety formulation, Y-PER™ (Fisher), listed as being a detergent based lysis reagent for yeast. This method is described to produce high levels of extracted protein without any kind of specialized equipment. However, due to the inherent necessity of using the supplied buffer, makes this a less flexible method, especially if one is to isolate protein in its native state.

Fig. 18 compares all four methods regarding the total protein extraction amounts, amount of ChR2 extracted and solubilized and information about time consumption scalability of the process.

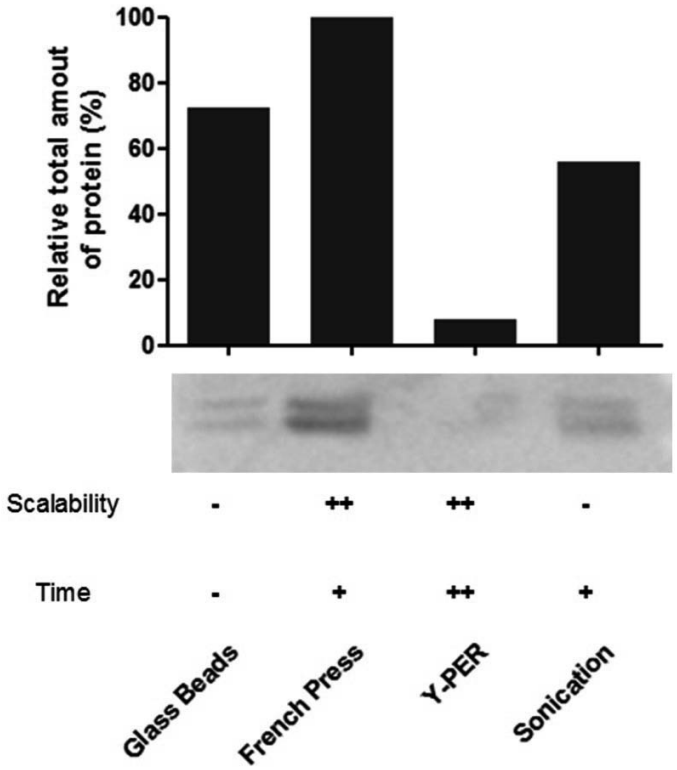

Figure 18 – Lysis methods comparison. Total amount of protein was determined and normalized to the highest yielding method (FrenchPress). After determining the total amount of protein, samples were normalized to 2mg/ml and western blot was made against the histidine tag present in the protein construct. Scalability and Time are presented in an arbitrary scale of performance (increasing from – to ++) based on the user's experience. These experiments were performed with equal contribution from Bruno Cruz and Fabio Mazza and the image here represented was chosen for its exemplary nature.

The French press system, when used at 7000 psi, is still the method that resulted in the highest amount of total protein extracted. It was followed by sonication and glass bead method with similar profiles, and Y-PER at the end of the efficiency curve. It is important to consider that although samples were highly diluted before quantification (>50 times), all the methods expect the Y-PER used the same homogenization buffer, whereas Y-PER didn't. It is possible that, due to interferences with the BCA method, detergents in the formulation interfered with the quantification and hence resulting in such low yields. Regardless, due to the nature of our work, we preferred not to use this reagent since we did not know to what extent the formulation would affect the successful purification of the protein.

Interestingly, French Press not only produced the highest amount of total protein extracted but appears to have the highest amount of non-aggregated protein as seen in the western blot membrane. Although all the samples were normalized to the same

concentration, glass beads and sonication result in loss of signal, most likely due protein aggregation that, at least for sonication, is a known phenomenon[78].

For all the reasons mentioned above we opt to use the pressure system in our experiments.

IV.5 – ChR2 purification by Nickel Affinity Chromatography

Upon confirming the expression of protein using *P. pastoris*, membrane fraction solubilized with n-Dodecyl β-D-maltoside (DDM), a detergent previously used to stabilize the protein in study[16,34,71] as well as other similar membrane proteins[1,79].

After obtaining the solubilized membrane fraction, the protein was purified using nickel affinity chromatography. Our initial loading buffer formulation[71] included: 20mM HEPES; 100mM NaCl, 10% (v/v) glycerol, 0,03% (w/v) DDM and 250mM Arginine. We optimized the buffer composition to maximize the purity of the protein. We opted to change the HEPES buffer to a phosphate buffer, as this was advised by the resin manufacturer, we also increased the concentration of salt and imidazole to reduce the non-specific protein binding[80,81] and decreased the concentration of glycerol due to excessive pressure on the column. The final result is represented in Fig.19.

In the silver staining gel it is possible to identify the same double band patter as in the previous western blots, with few contaminants, later confirmed by western blot of the same samples. Because of the nature of the assays needed to be performed after the purification, we chose not perform any further optimization since the chances that these contaminants present significant absorbance in the 300-800nm window is very small. Unfortunately, the amount of protein was too low to be observed by coomassie staining. This is in agreement with the low absorbance increase in the chromatogram probably due to low ChR2 concentration.

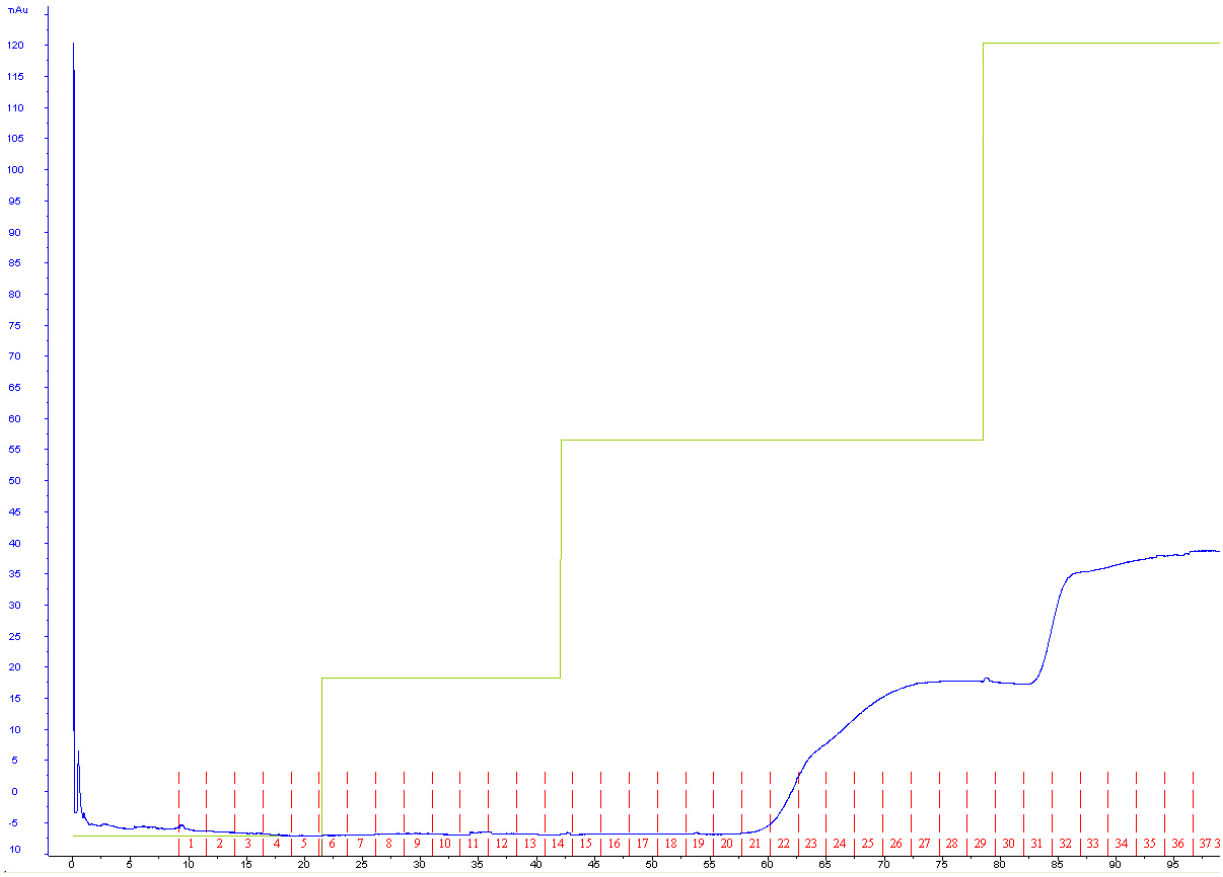
mAu
120
115
110
105
100
95
90
85
80
75
70
65
60
55
50
45
40
35
30
25
20
15
10
5
0
-5
10
0 5 10 15 20 25 30 35 40 45 50 55 60 65 70 75 80 85 90 95
1 2 3 4 5 6 7 8 9 10 11 12 13 14 15 16 17 18 19 20 21 22 23 24 25 26 27 28 29 30 31 32 33 34 35 36 37

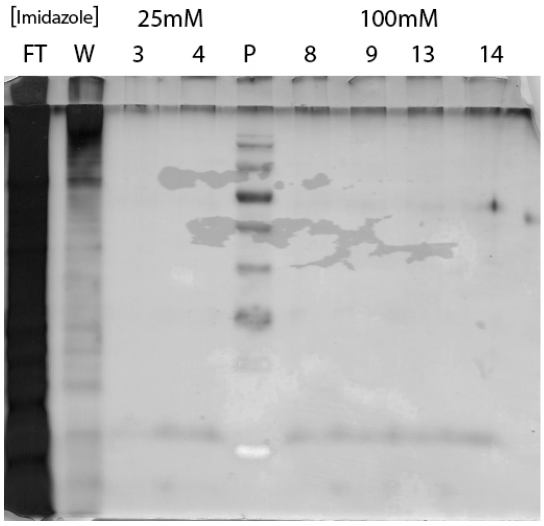
[Imidazole]
25mM
100mM
FT W 3 4 P 8 9 13 14

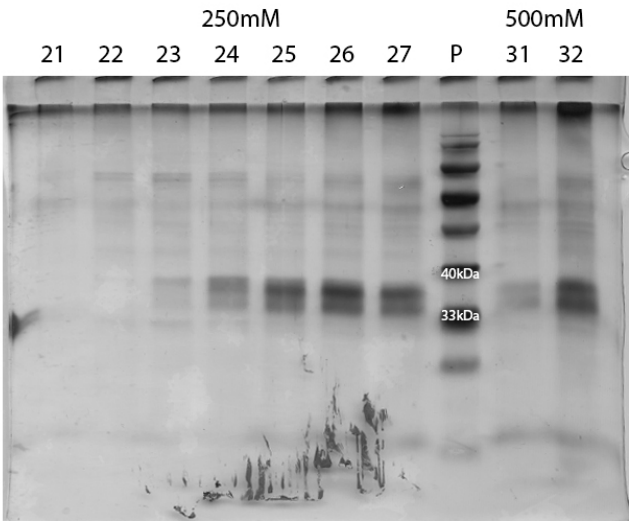
250mM
500mM
21 22 23 24 25 26 27 P 31 32
40kDa
33kDa

Figure 19 – ChR2-WT purification using nickel affinity chromatography. Top) Representative chromatogram of ChR2 purification. Blue = Absorbance at 260nm (A.U.); Green = Imidazole concentration (A.U. see methods); Red : Collected fractions (1.7mL each). Bottom) Silver Staining of selected chromatogram samples. FT= flowthrough; W=wash. Concentration of imidazole in mM.

Due to the high concentration of imidazole required to elute the protein from the column, dialysis was performed followed by protein concentration. For this, several samples were pooled together (from 250mM and 500mM imidazole). After the last step of protein purification, the amount of protein was insufficient to yield an absorption spectra as previously determined by other groups.

IV.6 – ChR2 protein expression in *Pichia pastoris X33 vs SMD1168H* strain

Having shown that ChR2 protein can be purified from *P. pastoris* and before applying the same protocols to our mutant versions, we aimed at obtaining higher amounts of protein. Towards this, we looked to the literature for other potential improvements to our protocol. Other groups that have successfully expressed ChR2 in *P.pastoris* have used proteinase A (pep4) deficient strains as expression system. However, in our first experiments we used the X33 strain, the wild-type strain as supplied by Invitrogen. Additionally, previous papers reported the low expression levels of ChR1 in this strain[82,51]

As a result we tried to repeat the previous experiments using a proteinase A deficient strain (SMD1168H). Fig.20 compares the expression of our originally selected clone for ChR2 from X33 strain to 5 colonies obtained from a 1000ug/ml Zeocin plate using the SMD1168H strain.

As it is observable in the western blot, even though there is some variability among SMD1168H colonies, the X33 clone achieves much higher expression levels of channelrhodopsin than any of the other SMD1168H.

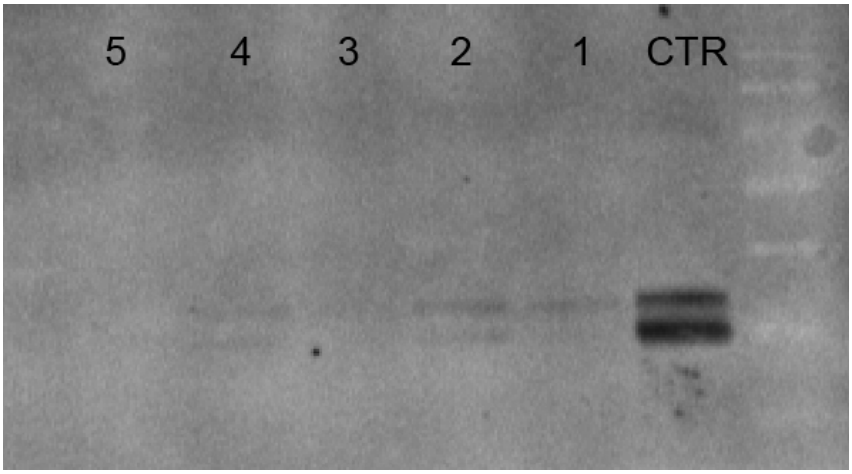

Figure 20 – ChR2 expression in P.pastoris X33 versus SMD1168H strains. CTR- Selected X33 strain used in the previous studies; 1-5 clones obtained from a single 1000ug/ml Zeocin YPD plate after a single electroporation. The volume loaded in the wells was normalized according to the cell pellet weight

Because of time constrains we could only repeat the electroporation process a second time, with the same results. Possible explanations for this outcome might be related to the small number of colonies screened. The possibility that we are comparing a “jackpot” clone from the X33 strain (which can present a tenfold increase in the protein expression)[69] against “normal” SMD1168H clones. On the other hand, other reports have described the pep4 deficient strain as less vigorous and harder to transform relative to X33. Because we used the simplest method for the preparation of electrocompetent cells, further optimization might be required to obtain similar or higher integration in this modified strain. Such protocols involve the use of more complex buffers that increase the transformation and viability rates of the electroporation process[69].

IV.7 – High-throughput ChR2 absorption spectra determination

Due to the nature of this work, the rate-limiting step is the expression and purification of the protein. By expression the protein in HEK293T cells, we sought to develop a method to screen several mutants in a short amount of time. Thus, after transfection and cell suspension we obtained the spectra depicted in Fig.21.

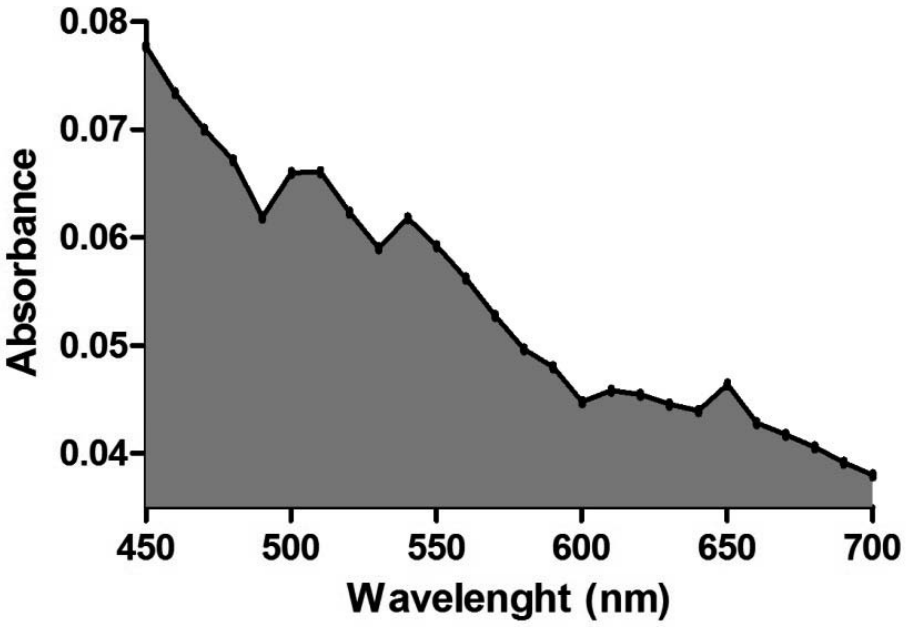

Figure 21 – Absorption spectra of ChR2-YFP transfected HEK293T cell. Cells were transfected with ChR2-YFP or with DNA elution buffer as a negative control. The curve results from the subtraction between ChR2-YFP and CTR cells. Number of cells was normalized before measurements.

In the present figure we can identify a peak near the maximum absorption wavelength of ChR2. However, this is most likely from eYFP which absorbs maximally at 514nm hence masking any potential signal from ChR2. In order to validate this

method we should construct a plasmid lacking eYFP and compare the non-transfected control against the ChR2 cell extract. If we can indeed detect the signal from ChR2, by generating several mutants and transfecting cell lines that are known to produce functional opsin, we can, at least in a preliminary fashion, triage several variants that produce the desired red-shifted behavior.

IV.8 – ChR2 membrane trafficking experiments

As mentioned above, previous studies have identified channelrhodopsins as highly aggregation prone proteins when expressed in mammalian systems.

To access the targeting of the mutants relative to wild-type ChR2 to the membrane, confocal imaging of transfected HEK293T cells was used (Fig.22).

As expected, WT ChR2 appears to have a clear membrane profile in contrast to cytoplasmic expression of YFP (CTR). Moreover, both mutations seem to have a clear membrane expression pattern, in spite of L183D mutation presenting a small degree of aggregation when compared against WT and F179D mutation. However, further studies need to be performed, especially electrophysiology experiments, to determine the functional properties of these mutations.

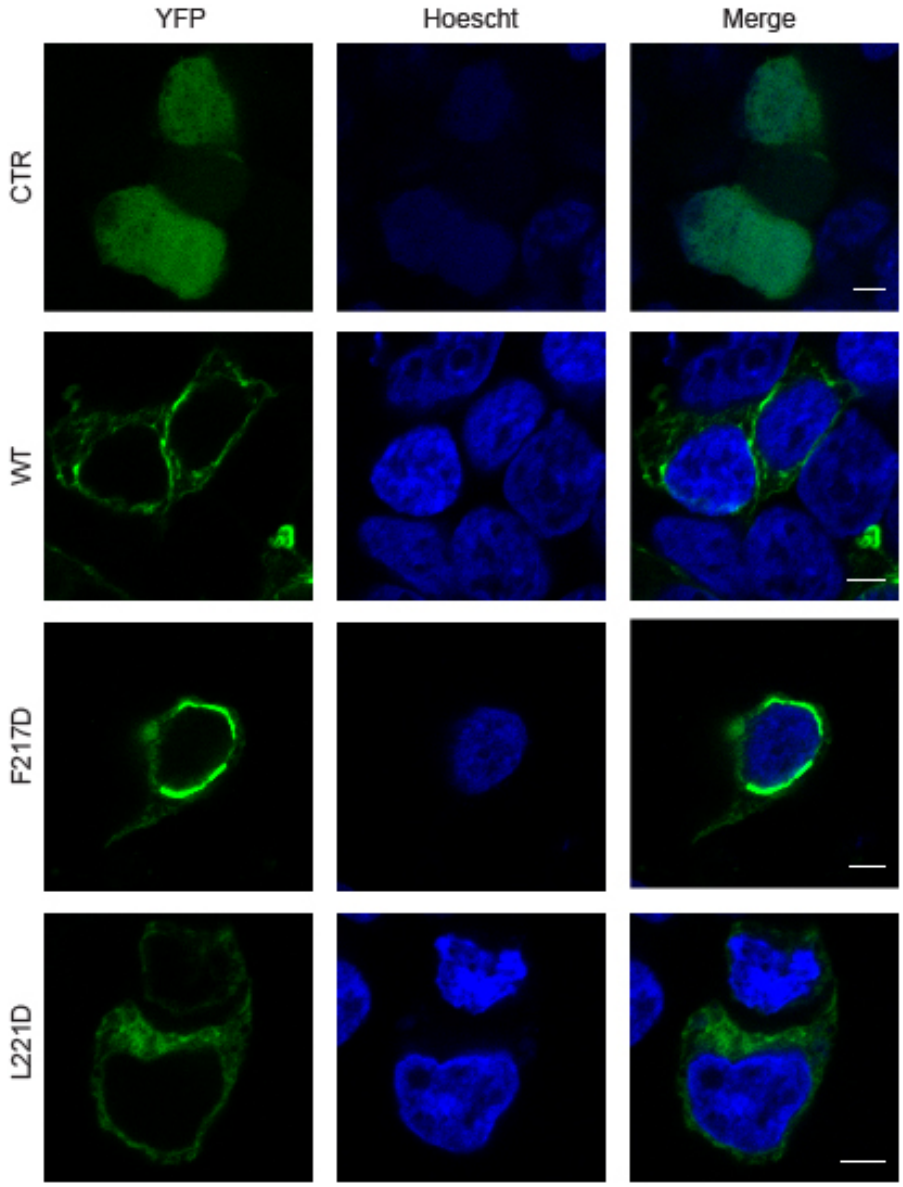

Figure 3 – Confocal imaging of ChR2 WT and mutants expression profile in HEK293T cells. Cells were transfected with lipofectamine LTX and expressed the protein for 24hours prior to fixation. Green= YFP; Blue = Hoescht staining. Control (CTR) is YFP vector which present a cytoplasmic expression. Scale bar = 5µm

Chapter V – General discussion and future directions

General Discussion and future directions

Optogenetic approaches have revolutionized the field of neuroscience. For the first time it is possible to reliably achieve activation or inhibition of genetically targeted cells by light delivery. This allows researchers to probe the nervous system, from single cell to the circuit level, with a resolution previously unattainable. Although much effort has been put into expanding the optogenetic actuator's toolbox repertoire, there is considerable room for improvement. This is especially true when it comes to a red-shifted actuator capable of inducing neuronal depolarization with similar proprieties as the original ChR2.

In this work we report the possibility of generating color-tuned variants of ChR2, by directed-site mutagenesis, using computational methods to predict the change in the absorption spectra on the protein.

Presently, two mutants were generated that are predicted to result into a red-shift of 65 and 40nm, respectively. Even though it is unlikely that these two mutations will be enough to generate a mutant with non-overlapping absorption spectra relative to other variants, using the same rational behind their manipulation, these might present as a strategy for an incremental generation of other color-tuned mutants. More importantly, it is probable that to generate a greater shift, insertion of more than a single mutation might be necessary, as a result it is in our interest to identify as many mutants as possible. At the same time, the spectral characterization of each mutation may be used to refine the TD-DFT model in an iterative process.

To generate these mutants we successfully applied a directed-site mutagenesis strategy and constructed vectors ready to use in mammalian systems.

In order to validate the predictions of Octopus algorithm we sought to express and purify ChR2 from *Pichia pastoris*. We optimized the overall strategy of purification for Wt-ChR2 which will likely be applied to other mutants without any further optimization, since single or higher order modifications in the primary structure of the protein do not seem to alter its structure to a great degree, making it unlikely to affect the purification protocol in any significant way. In spite of successfully purifying the protein, its amount was not sufficient to perform a spectroscopic read-out, as a result the TD-DFT predictions remain to be confirmed. To solve this issue we can propose several solutions, namely: scaling up the culture system and performing several rounds of proteins concentration, screening for additional clones, optimizing expression conditions using adjuvants such as DMSO or varying concentrations of methanol, optimizing the electroporation and expression in the SMD1168H strain, among others.

Regarding the protein behavior in its “native” environment, we proved that both wild-type ChR2 and the presented variants appear to have a strong membrane targeting profile without showing extensive aggregation, supporting that hypothesis that our insertion of modifications in the primary structure of the protein did not alter its overall folding to a great extent.

Although not a part of the result section of this thesis, we also tried to electrophysiologically characterize the channel by expressing the protein into neuron and HEK293T cells as previously described[40,49]. For that we integrated a light delivery system into standard patch-clamp electrophysiology equipment and tried to determine

kinetic constants of the channel, because, although one can obtain a red-shifted opsin from manipulations previously done, it is possible that, unintentionally, we affected the kinetic proprieties of the channel. Unfortunately, due to time constrains, we only succeeding in optimizing the cell seeding procedure and several of the system settings.

The conclusion of this work might prove seminal to the generation of color-tuned ChR2 as well as application of the same rational to other molecules.

Chapter VI – References

References

1. Palczewski, K. G protein-coupled receptor rhodopsin. *Annu. Rev. Biochem.* **75,** 743–67 (2006).

2. Zhang, F. *et al.* The microbial opsin family of optogenetic tools. *Cell* **147,** 1446–57 (2011).

3. Hegemann, P. & Nagel, G. From channelrhodopsins to optogenetics. *EMBO Mol. Med.* **5,** 173–6 (2013).

4. Schaller, K., David, R. & Uhl, R. How Chlamydomonas keeps track of the light once it has reached the right phototactic orientation. *Biophys. J.* **73,** 1562–72 (1997).

5. Foster, K. W. & Smyth, R. D. Light Antennas in phototactic algae. *Microbiol. Rev.* **44,** 572–630 (1980).

6. Harz, H. & Hegemann, P. Rhodopsin-regulated calcium currents in Chlamydomonas. *Nature* **351,** 489–491 (1991).

7. Herrmann, T. R. & Rayfield, G. W. A measurement of the proton pump current generated by bacteriorhodopsin in black lipid membranes. *Biochim. Biophys. Acta* **443,** 623–8 (1976).

8. Nagel, G., Möckel, B., Büldt, G. & Bamberg, E. Functional expression of bacteriorhodopsin in oocytes allows direct measurement of voltage dependence of light induced H+ pumping. *FEBS Lett.* **377,** 263–6 (1995).

9. Nagel, G. *et al.* Channelrhodopsin-1: a light-gated proton channel in green algae. *Science* **296,** 2395–8 (2002).

10. Nagel, G. *et al.* Channelrhodopsin-2, a directly light-gated cation-selective membrane channel. *Proc. Natl. Acad. Sci. U. S. A.* **100,** 13940–5 (2003).

11. Witman, G. B. Chlamydomonas phototaxis. *Trends Cell Biol.* **3,** 403–8 (1993).

12. Bruegmann, T. *et al.* Optogenetic control of heart muscle in vitro and in vivo. *Nat. Methods* **7,** 897–900 (2010).

13. Deisseroth, K. *et al.* Next-generation optical technologies for illuminating genetically targeted brain circuits. *J. Neurosci.* **26,** 10380–6 (2006).

14. Boyden, E. S., Zhang, F., Bamberg, E., Nagel, G. & Deisseroth, K. Millisecond-timescale, genetically targeted optical control of neural activity. *Nat. Neurosci.* **8,** 1263–8 (2005).

15. Miesenböck, G. Optogenetic control of cells and circuits. *Annu. Rev. Cell Dev. Biol.* **27,** 731–58 (2011).

16. Kato, H. E. *et al.* Crystal structure of the channelrhodopsin light-gated cation channel. *Nature* **482,** 369–74 (2012).

17. Lin, J. Y. A user's guide to channelrhodopsin variants: features, limitations and future developments. *Exp. Physiol.* **96,** 19–25 (2011).

18. Zhao, S. *et al.* Improved expression of halorhodopsin for light-induced silencing of neuronal activity. *Brain Cell Biol.* **36,** 141–54 (2008).

19. Klapoetke, N. C. *et al.* Independent optical excitation of distinct neural populations. *Nat. Methods* **11,** 338–46 (2014).

20. Zhang, F. *et al.* Optogenetic interrogation of neural circuits: technology for probing mammalian brain structures. *Nat. Protoc.* **5,** 439–56 (2010).

21. Hegemann, P. & Möglich, A. Channelrhodopsin engineering and exploration of new optogenetic tools. *Nat. Methods* **8,** 39–42 (2011).

22. Watanabe, H. C. *et al.* Structural model of channelrhodopsin. *J. Biol. Chem.* **287,** 7456–66 (2012).

23. Loppnow, G. R., Barry, B. A. & Mathies, R. A. Why are blue visual pigments blue? A resonance Raman microprobe study. *Proc. Natl. Acad. Sci. U. S. A.* **86,** 1515–8 (1989).

24. Wang, W. *et al.* Tuning the electronic absorption of protein-embedded all-trans-retinal. *Science* **338,** 1340–3 (2012).

25. Okada, T. *et al.* The retinal conformation and its environment in rhodopsin in light of a new 2.2 A crystal structure. *J. Mol. Biol.* **342,** 571–83 (2004).

26. Nishikawa, T., Murakami, M. & Kouyama, T. Crystal structure of the 13-cis isomer of bacteriorhodopsin in the dark-adapted state. *J. Mol. Biol.* **352,** 319–28 (2005).

27. Müller, M., Bamann, C., Bamberg, E. & Kühlbrandt, W. Projection structure of channelrhodopsin-2 at 6 Å resolution by electron crystallography. *J. Mol. Biol.* **414,** 86–95 (2011).

28. Catterall, W. a. Structure and function of voltage-gated ion channels. *Annu. Rev. Biochem.* **64,** 493–531 (1995).

29. Eisenhauer, K. *et al.* In channelrhodopsin-2 Glu-90 is crucial for ion selectivity and is deprotonated during the photocycle. *J. Biol. Chem.* **287,** 6904–11 (2012).

30. Plazzo, A. P. *et al.* Bioinformatic and mutational analysis of channelrhodopsin-2 protein cation-conducting pathway. *J. Biol. Chem.* **287,** 4818–25 (2012).

31. Watanabe, H. C., Welke, K., Sindhikara, D. J., Hegemann, P. & Elstner, M. Towards an understanding of channelrhodopsin function: simulations lead to novel insights of the channel mechanism. *J. Mol. Biol.* **425,** 1795–814 (2013).

32. Ritter, E., Stehfest, K., Berndt, A., Hegemann, P. & Bartl, F. J. Monitoring light-induced structural changes of Channelrhodopsin-2 by UV-visible and Fourier transform infrared spectroscopy. *J. Biol. Chem.* **283,** 35033–41 (2008).

33. Bamann, C., Kirsch, T., Nagel, G. & Bamberg, E. Spectral characteristics of the photocycle of channelrhodopsin-2 and its implication for channel function. *J. Mol. Biol.* **375,** 686–94 (2008).

34. Stehfest, K., Ritter, E., Berndt, A., Bartl, F. & Hegemann, P. The branched photocycle of the slow-cycling channelrhodopsin-2 mutant C128T. *J. Mol. Biol.* **398,** 690–702 (2010).

35. Stryer, L. Cyclic GMP cascade of vision. *Annu. Rev. Neurosci.* **9,** 87–119 (1986).

36. Arenkiel, B. R. *et al.* In vivo light-induced activation of neural circuitry in transgenic mice expressing channelrhodopsin-2. *Neuron* **54,** 205–18 (2007).

37. Zhang, F. *et al.* Red-shifted optogenetic excitation: a tool for fast neural control derived from Volvox carteri. *Nat. Neurosci.* **11,** 631–3 (2008).

38. Berndt, A., Yizhar, O., Gunaydin, L. a, Hegemann, P. & Deisseroth, K. Bi-stable neural state switches. *Nat. Neurosci.* **12,** 229–34 (2009).

39. Perálvarez-Marín, A., Márquez, M., Bourdelande, J.-L., Querol, E. & Padrós, E. Thr-90 plays a vital role in the structure and function of bacteriorhodopsin. *J. Biol. Chem.* **279,** 16403–9 (2004).

40. Yizhar, O. *et al.* Neocortical excitation/inhibition balance in information processing and social dysfunction. *Nature* **477,** 171–8 (2011).

41. Nack, M. *et al.* The DC gate in Channelrhodopsin-2: crucial hydrogen bonding interaction between C128 and D156. *Photochem. Photobiol. Sci.* **9,** 194–8 (2010).

42. Berndt, A., Lee, S., Ramakrishnan, C. & Deisseroth, K. Structure-Guided Transformation of Channelrhodopsin into a Light-Activated Chloride Channel. *Science (80-.).* **344,** 420–424 (2014).

43. Yizhar, O., Fenno, L. E., Davidson, T. J., Mogri, M. & Deisseroth, K. Optogenetics in neural systems. *Neuron* **71,** 9–34 (2011).

44. Gunaydin, L. A. *et al.* Ultrafast optogenetic control. *Nat. Neurosci.* **13,** 387–392 (2010).

45. Yizhar, O., Fenno, L. E., Davidson, T. J., Mogri, M. & Deisseroth, K. Optogenetics in neural systems. *Neuron* **71,** 9–34 (2011).

46. Govorunova, E. G., Spudich, E. N., Lane, C. E., Sineshchekov, O. A. & Spudich, J. L. New channelrhodopsin with a red-shifted spectrum and rapid kinetics from Mesostigma viride. *MBio* **2,** e00115–11 (2011).

47. Rein, M. L. & Deussing, J. M. The optogenetic (r)evolution. *Mol. Genet. Genomics* **287,** 95–109 (2012).

48. Chen, Q., Zeng, Z. & Hu, Z. Optogenetics in neuroscience: what we gain from studies in mammals. *Neurosci. Bull.* **28,** 423–34 (2012).

49. Lin, J. Y., Lin, M. Z., Steinbach, P. & Tsien, R. Y. Characterization of engineered channelrhodopsin variants with improved properties and kinetics. *Biophys. J.* **96,** 1803–14 (2009).

50. Gradinaru, V. *et al.* Molecular and cellular approaches for diversifying and extending optogenetics. *Cell* **141,** 154–65 (2010).

51. Hou, S. Homology Cloning, Heterologous Expression and Characterization of a New Channelrhodopsin. (2012). at <http://digitalcommons.library.tmc.edu/utgsbs_dissertations/326/>

52. Bamann, C., Gueta, R., Kleinlogel, S., Nagel, G. & Bamberg, E. Structural guidance of the photocycle of channelrhodopsin-2 by an interhelical hydrogen bond. *Biochemistry* **49,** 267–78 (2010).

53. Macauley-Patrick, S., Fazenda, M. L., McNeil, B. & Harvey, L. M. Heterologous protein production using the Pichia pastoris expression system. *Yeast* **22,** 249–70 (2005).

54. Ramón, A. & Marín, M. Advances in the production of membrane proteins in Pichia pastoris. *Biotechnol. J.* **6,** 700–6 (2011).

55. Higgins, D. R. Overview of protein expression in Pichia pastoris. *Curr. Protoc. Protein Sci.* **Chapter 5,** Unit5.7 (2001).

56. Beckwith, J. Fifty years fused to lac. *Annu. Rev. Microbiol.* **67,** 1–19 (2013).

57. Balamurugan, V. Pichia pastoris: A notable heterologous expression system for the production of foreign proteins-Vaccines. *Indian J. …* **6,** 175–186 (2007).

58. Daly, R. & Hearn, M. T. W. Expression of heterologous proteins in Pichia pastoris: a useful experimental tool in protein engineering and production. *J. Mol. Recognit.* **18,** 119–38 (2005).

59. Burke, K., Werschnik, J. & Gross, E. K. U. Time-dependent density functional theory: past, present, and future. *J. Chem. Phys.* **123,** 62206 (2005).

60. Kohn, W. & Sham, L. J. Self-Consistent Equations Including Exchange and Correlation Effects. *Phys. Rev.* **140,** A1133–A1138 (1965).

61. Andrade, X. *et al.* Time-dependent density-functional theory in massively parallel computer architectures: the OCTOPUS project. *J. Phys. Condens. Matter* **24,** 233202 (2012).

62. Castro, A. *et al.* octopus: a tool for the application of time-dependent density functional theory. *Phys. status solidi* **243,** 2465–2488 (2006).

63. Marques, M. octopus: a first-principles tool for excited electron–ion dynamics. *Comput. Phys. Commun.* **151,** 60–78 (2003).

64. Varsano, D., Di Felice, R., Marques, M. A. L. & Rubio, A. A TDDFT study of the excited states of DNA bases and their assemblies. *J. Phys. Chem. B* **110,** 7129–38 (2006).

65. Milne, B. F., Marques, M. A. L. & Nogueira, F. Fragment molecular orbital investigation of the role of AMP protonation in firefly luciferase pH-sensitivity. *Phys. Chem. Chem. Phys.* **12,** 14285–93 (2010).

66. Marques, M., López, X., Varsano, D., Castro, A. & Rubio, A. Time-Dependent Density-Functional Approach for Biological Chromophores: The Case of the Green Fluorescent Protein. *Phys. Rev. Lett.* **90,** 258101 (2003).

67. Hamilton, R., Watanabe, C. K. & de Boer, H. A. Compilation and comparison of the sequence context around the AUG startcodons in Saccharomyces cerevisiae mRNAs. *Nucleic Acids Res.* **15,** 3581–3593 (1987).

68. Schowen, R. L. Principles of biochemistry 2nd ed. (Lehninger, Albert L.; Nelson, David L.; Cox, Michael M.). *J. Chem. Educ.* **70,** A223 (1993).

69. Cregg, J. M. *et al. Expression in the yeast Pichia pastoris. Methods Enzymol.* **463,** 169–89 (Elsevier Inc., 2009).

70. Lórenz-Fonfría, V. a *et al.* Transient protonation changes in channelrhodopsin-2 and their relevance to channel gating. *Proc. Natl. Acad. Sci. U. S. A.* **110,** E1273–81 (2013).

71. Bruun, S. *et al.* The chromophore structure of the long-lived intermediate of the C128T channelrhodopsin-2 variant. *FEBS Lett.* **585,** 3998–4001 (2011).

72. Ernst, O. P. *et al.* Microbial and animal rhodopsins: structures, functions, and molecular mechanisms. *Chem. Rev.* **114,** 126–63 (2014).

73. Lorenz-Fonfria, V. a & Heberle, J. Channelrhodopsin unchained: Structure and mechanism of a light-gated cation channel. *Biochim. Biophys. Acta* (2013). doi:10.1016/j.bbabio.2013.10.014

74. Lin, S.-H. & Guidotti, G. *Purification of membrane proteins. Methods Enzymol.* **463,** 619–29 (Elsevier Inc., 2009).

75. Ernst, O. P. *et al.* Photoactivation of channelrhodopsin. *J. Biol. Chem.* **283,** 1637–43 (2008).

76. Lipke, P. & Ovalle, R. Cell wall architecture in yeast: new structure and new challenges. *J. Bacteriol.* **180,** (1998).

77. Feliu, J. X., Cubarsi, R. & Villaverde, a. Optimized release of recombinant proteins by ultrasonication of E. coli cells. *Biotechnol. Bioeng.* **58,** 536–40 (1998).

78. Stathopulos, P. B. *et al.* Sonication of proteins causes formation of aggregates that resemble amyloid. 3017–3027 (2004). doi:10.1110/ps.04831804.Protein

79. Filipek, S., Stenkamp, R. E., Teller, D. C. & Palczewski, K. G protein-coupled receptor rhodopsin: a prospectus. *Annu. Rev. Physiol.* **65,** 851–79 (2003).

80. Block, H. *et al.* Immobilized-metal affinity chromatography (IMAC): a review. *Methods Enzymol.* **463,** 439–73 (2009).

81. Bornhorst, J. & Falke, J. Purification of proteins using polyhistidine affinity tags. *Methods Enzymol.* (2000). at <http://www.sciencedirect.com/science/article/pii/S0076687900260588/pdf?md5=d3e71cf0b9b5870ade6f3b850f65ce5b&pid=1-s2.0-S0076687900260588-main.pdf&_valck=1>

82. Berthold, P. *et al.* Channelrhodopsin-1 initiates phototaxis and photophobic responses in chlamydomonas by immediate light-induced depolarization. *Plant Cell* **20,** 1665–77 (2008).